BRNO UNIVERZITY OF TECHNOLOGY

FACULTY OF CHEMISTRY

DEPARTMENT OF THE MATERIAL SCIENCE

Ing. Soňa Kontárová

Nanolayered composites

Nanovrstevnaté kompozity

(short version of Doctoral Thesis)

Branch:	Chemistry, Technology and Properties of Materials
Leader:	Prof. RNDr. Vladimír Čech, PhD.
Opponents:	Doc. Ing. Ota Salyk, CSc. Dr. Mgr. Jan Mistrík, PhD.
Date of vindication:	24.3. 2011

Key Words

plasma polymerization, multilayers, tetravinylsilane, thin films, ellipsometry

Klíčová Slova

plazmová polymerizace, multivrstvy, tetravinylsilan, tenké vrstvy, elipsometrie

The location of work storage

The library of Faculty of Chemistry, BUT in Brno

ISBN 80-214-
ISSN 1213-4198

CONTENTS

1 INTRODUCTION

Plasma was first recognized as “radiant matter” in a Crook tube and described by Sir William Crookes in 1789 and first notes about deposits known today as plasma polymers appeared in the second half of the 19th century. The term “plasma” was first established by Irving Langmuir in 1928. Langmuir wrote: Except near the electrodes, where there are sheaths containing very few electrons, the ionized gas contains ions and electrons in about equal numbers so that the resultant space charge is very small. We shall use the name plasma to describe this region containing balanced charges of ions and electrons [1].

Plasma polymers in most cases were recognized as undesirable by-products of phenomena associated with electric discharge; hence little attention was paid to the properties of these materials or to the process for forming useful materials. As far as 1960s was the formation of materials in plasma recognized for synthesizing polymers, the process useful for making a special coating on metals, has been named to as plasma polymerization or glow discharge polymerization. Plasma polymerization today is an important process for the formation of entirely new kinds of materials, which are significantly different from conventional polymers and most inorganic materials [2]. Plasma polymerization benefits are capability to polymerize almost every organic matter, high deposition rate and the preparation of thin films without defects.

Plasma polymerization process started to be investigated due to many potential applications e.g. in electrical and optical fields and surface modifications especially for biomedical applications [3-6]. The most important forms of plasma polymers are ultrathin films. Meaningful plasma applications are namely e.g. barrier coatings for the corrosion protection of metals [7], barrier coatings protecting food against oxygen and water vapor in packaging technology [8, 9], thin films protecting automobile components against friction [10], thin films improving ‘biocompatibility’ of vascular prostheses, heart valves, intra-ocular and contact lenses [11, 12]. Important are thin layers with low dielectric constant (low-*k* materials) improving integration in microchips, decreasing the signal propagation delay and cross-talk and wide-spread used in microelectronics as insulators [13-16]. Thin films can be also used in green chemistry, e.g. as hydrophobic layers on biologically degradable polymeric foils [17].

Plasma enhanced chemical vapor deposition (PE-CVD) is a suitable technique for preparation of thin films on a basis of organosilicones, e.g. vinyltriethoxysilane films and tetravinylsilane films with oxygen. Reproducible deposition of plasma polymer films with desired physical-chemical properties is enabled by changing the deposition conditions, especially effective power, pressure, and monomer flow rate. Such a film of organic/inorganic character could be used as a compatible interlayer for multicomponent materials such as nanocomposites and fiber-reinforced polymer composites.

To eliminate or at least reduce the internal stresses and improve adhesion, mostly multilayered rather than a single layered film has to be used. Such multilayers may be used for passivation of organic devices [18], as a dielectric barrier in semiconductor devices [19], as tribological coating in aeronautical applications [20], or as functional coating in polymer composites with controlled interphase [21]. Optical films based on multilayer structures as well as inhomogeneous coatings with gradually varied refractive index have many important applications, such as antireflective coating, optical filters and integrated optical devices [22].

This study is aimed at the basic research of plasma polymer films and an influence of deposition conditions on structure and properties of single-layer films and multilayers prepared by PE CVD method. Single layer and multilayered a-SiCO:H films were deposited on silicon wafers from tetravinylsilane monomer (TVS) at different powers in continual and pulse regimes. Films were investigated intensively by spectroscopic ellipsometry, nanoindentation, atomic force microscopy (AFM), X-ray photoelectron spectroscopy (XPS), Rutherford Backscattering Spectrometry (RBS), X-ray reflectivity, Fourier Transform Infrared Spectroscopy (FTIR) and contact angle measurements to investigate their optical, mechanical and chemical properties. The influence of the deposition condition on the physico-chemical properties of pp-layers was investigated and proved. Single layers were also exposed to UV light to investigate aging effects and the influence of UV irradiation on their physical and chemical properties. In this short version of doctoral thesis, only the most important and chosen results are presented.

2 EXPERIMENTAL PART

2.1 PLASMA POLYMERIZATION

2.1.1 Materials and working gases

Tetravinylsilane (TVS) was used as the monomer for the plasma-polymerized films, and has been chosen due to the presence of vinyl groups and absence of oxygen. Monomer is embedded in the thermostatic bath in a liquid form, but for deposition only monomer vapors are flushed into the plasma reactor.

Tetravinylsilane (TVS):
Molecular formula: $Si(-HC=CH_2)_4$
Purity: 97 %
Molecular weight: 136.27 g/mol
Density: 0.8 g/cm^3
Boiling-point: 130 – 131 °C
Refractive index: 1.461

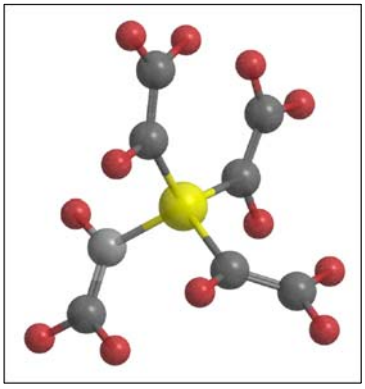

Figure 1: Tetravinylsilane (TVS)

Argon gas (Linde gas, purity 99.999 %) was employed as a working gas for cleaning of the plasma reactor, pretreatment and deposition of films. Oxygen gas (Linde gas, purity 99.995 %) was in some cases used for plasma treatment of the plasma polymerized TVS films.

Infrared-transparent double-polished silicon wafers {0.6 × 10 × 10 mm^3, with impurity max. 6.9 – 8.9 × 10^{17} at·cm^{-3}, configuration (100), On Semiconductor, s.r.o., Czech Republic} were chosen as wafers because of high number of required thin film analyses (RBS, XPS, FTIR and ellipsometry measurements).

Special microscope slides without flaws were used as alternative substrates (1.0 × 26 × 76 mm^3, refractive index n = 1.518, Knittel Gläser, Germany). These substrates were used only for the free surface energy determination of prepared plasma-polymeric layers.

2.1.2 Deposition apparatus

The plasma system (Figure 2) with working label “A3” is aimed at the preparation of functionally nanostructured thin films with high reproducibility. This plasma reactor has been developed within the scope of the joint Czech-Japan project (2002-2004) supported by the Czech and Japan Ministry of Education. All parts of the vacuum device are made from the stainless steel, connected by copper vacuum seals or vacuum “O-rings” from Viton (fluorinated elastomer, DuPont Company). The internal setup of our deposition chamber, using plan-parallel electrodes, was derived

from a typical capacitive coupling system, but our apparatus uses novel creative design and is equipped with many non-standard components [23].

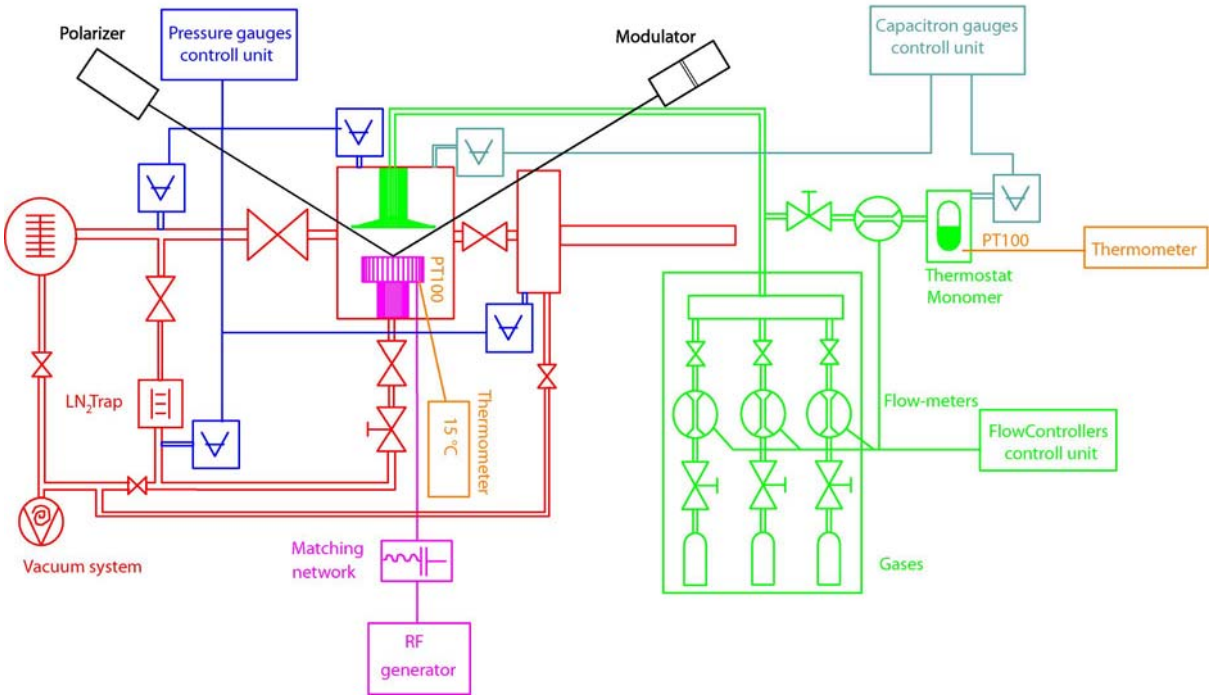

Figure 2: Schematic illustration of technological apparatus "A3" [23]

The main part of the device consist of a cylindrical reactor (25 × 25 cm). The reactor is equipped inside with two plan-parallel copper OFHC (Oxygen Free High Conductivity) electrodes. A special construction of bottom rotary electrode (ø 114 mm) enabled us to switch up to 6 samples into/from the reactor chamber under vacuum, avoiding reactor contamination because device uses a magnetic drive (linear and rotary, BOC Edwards) and a special load lock mounted inside of differentially pumped side chamber. The rotary electrode can also be selectively heated or cooled ranging from –100 to 300 °C. The RF power from generator output is applied on the bottom electrode through the matching network. The matching network consists of tunable LC circuit. The upper electrode (ø 135 mm) of shower-type is grounded and can be positioned in a distance of 20 – 60 mm from the bottom one. The working gases and monomer are fed into the reactor through this electrode. A movable substrate shutter can be used to deposit film at steady-state plasma conditions and can be positioned between the upper and bottom electrodes.

A turbomolecular pump (TMU 261 P, Pfeiffer Vacuum, pumping speed 170 l/s, rotating velocity 50 000 rpm[2]) with a dry scroll pump (TriScroll 300, Varian, pumping speed 210 l/min which serves to create the fore-vacuum as the first stage) and an LN_2-cooled trap were selected to evacuate the system in order to eliminate oil vapor, minimize water vapor content in all vacuum chambers and thus acquire the basic pressure ~ 10^{-6} Pa. Cleaning of the system, substrate pretreatment, and deposition process is automated via control unit [23 - 26]. The high vacuum is

acquired in the apparatus hence it is necessary to measure the pressure in the large range. The apparatus is equipped with eight pressure gauges for measurement of pressure in the whole system.

The reactor was equipped with mass spectrometer (Process Gas Analyzer HPR-30, Hiden Analytical), to monitor the reactor state and reaction processes during deposition, and by in-situ spectroscopic ellipsometer (UVISEL, Jobin Yvon), to monitor the optical properties of samples and film growth.

The plasma, namely the glow discharge is generated by an RF-generator (Cesar 1310, 13.56 MHz, 1000 W, Dressler) which is connected to the system using the automatic matching network (VM 1000A, Dressler). It is possible to achieve a range of effective power density from 1×10^{-4} to 4×100 W · cm^{-3} using pulsed plasma regime and 1×10^{-3} to 4×100 W · cm^{-3} in continuous regime relative to the movable top electrode. The RF-generator is controlled by the PC (personal computer) via control unit - the program "A3 controller", which is able to change fluently the RF-power and can switch between the continual and pulse regime. Pulses are generated internally by generator timer and can be changed in the wide range of frequencies and duty cycles, but at condition where minimally t_{ON} or t_{OFF} have value of 16 μs and duty cycle can be changed in the range of 1 – 99 % with step 1 %. The pulse regime provide customizable time intervals, t_{ON} when the RF-power is applied and t_{OFF} when the RF-power is not applied to the system. Period T or frequency f can be evaluated from the values of t_{ON} and t_{OFF} (Equations 1, 2).

$$T = t_{ON} + t_{OFF} \quad [s] \tag{1}$$

$$f = T^{-1} \quad [Hz] \tag{2}$$

The duty cycle of magnitude S is expressed for comparison of power delivered to the reactor in continual and pulse regime. The effective power of discharge P_{Eff} can be evaluated from this value (Equations 3, 4). Plasma depositions with same effective powers and different pulse frequencies can provide pp-layers with different physio-chemical properties. It is necessary to indicate not only the effective power, but also pulse frequency or t_{ON}.

$$S = \frac{t_{ON}}{t_{ON} + t_{OFF}} = \frac{t_{ON}}{T} \text{ or } S = 100 \cdot \frac{t_{ON}}{T} \quad [\%] \tag{3}$$

$$P_{Eff} = P_{Sp} \cdot S \quad [W] \tag{4}$$

where P_{Sp} is the real (supplied) power.

The apparatus is equipped with nine mostly pneumatic valves from VAT Company to control the gas flow. The working gases (argon, oxygen) and monomer vapor are fed through flow meters into the upper part of the reactor through

collective pipes – to the shower upper electrode, which is grounded. Digital flow meters (Bronkhorst Company) are applied to control gas dosage and measuring the volume of gas flow via the heat capacity of gas. Flow meter used for monomer flow rates can be changed arbitrarily in the range of 2 – 100 sccm and is calibrated for nitrogen gas. Thus it is necessary to establish calibrating curve dependency for the real monomer flow rate on the set up value. The monomer flow rates can be then optional in the range of 0 – 14 sccm.

2.1.3 Plasma polymerization and conditions

Our deposition technology and deposition procedures for preparation of thin plasma polymerized layers result not only from knowledge obtained from the literature [2, 27] but mainly from experimental experiences obtained during apparatus utilization.

Before deposition it is necessary to reach the certain purity of the deposition system which correspond to the pressure in the reactor chamber lower than the basic pressure $p_{bas} = 3 \times 10^{-5}$ Pa. If there is still problem reaching the basic pressure after long pumping time, it is necessary to check leaks of particular joints in the reactor, using the helium. Incidental leaks suck helium into the reactor where it can be identified using the mass spectrometer. The mass spectrometry also served for the purity control of the basic vacuum, to check for impurities present in the system or if there is atmospheric water condensate presents in the system (the condensate water can enter the system due to air locking, the sample loading and after the cleaning of the reactor). If the water is present in the reactor, it is possible to heat the bottom electrode and lateral area of the reactor up to 110 °C during pumping and that way to help the water desorption from the surface.

After the verification of the basic vacuum (the pressure in the reactor chamber is stable and under the value of $p_{bas} = 3 \times 10^{-5}$ Pa; reactor environment is clean after the control by mass spectroscopy), it is possible to start with deposition of thin polymer films. The deposition includes following basic steps. Initially the silicon surface is activated by the argon plasma, so the active radicals are created on the silicon surface to provide better adhesion and better link to the monomer fragments and radicals. After the activation, the plasma polymerization from the monomer vapors proceeds. It is necessary to retain the samples in the reactor under the vacuum in order to reduce free radicals after the plasma polymerization. The gases from the atmosphere could link to these free radicals during exposition on the atmosphere and thereby modify resulting plasma polymer. Accurate and reproducible deposition procedure, described in the Table 1 has been developed after the several variants and changes in the deposition system.

Table 1: Procedures for plasma polymer films preparation

1	*Loading samples into the bottom electrode in the reactor chamber*. At least 6 substrate holders are inserted into the load-lock reservoir and then load-lock seal has to be closed down. Using the magnetic linear drive, the substrate holders with samples are moved from the load-lock chamber to the rotary bottom electrode (electrode has to be fully filled because the plasma would not be homogeneous).
2	*Reactor chamber evacuation up to basic pressure* $p_{bas} = 3 \times 10^{-5}$ *Pa by the scroll and turbomolecular pump*.
3	*Monitoring of residual gases by mass spectroscopy*.
4	*The adjustment of the pumping flow rate by the butterfly valve*. 10 sccm of argon gas is flushed into the reactor by the flow meter. Using the A3 controller, the butterfly valve is strangulated on particular position in order to reach the pressure of 5 Pa in the reactor at the argon flow rate of 10 sccm. After some recent changes in the apparatus – the apparatus was equipped with steel meander, located in front of the butterfly valve and used for interception of undesirable particles of deposit – the butterfly valve is strangulated on the pressure 5.71 Pa at argon flow rate of 10 sccm to keep standard deposition condition.
5	*Monitoring of the argon gas purity by mass*.
6	*Argon-plasma pretreatment*. Using A3 controller, the generator input power is set up at 5 W in continual plasma regime. 10 sccm of argon gas is still flushed into the reactor. The plasma glow discharge is switched on for 10 minutes. The silicon surface is thus activated by Ar plasma. During plasma activation it is possible to measure optical parameters of sample by in-situ spectroscopic ellipsometry and check the running processes in the plasma by mass spectroscopy measurements.
7	*Reactor evacuating after argon activation for maximum time of 10 minutes*. Glow discharge is switched off, argon flow rate is stopped, reactor is evacuated on the basic pressure $P_{bas} = 3 \times 10^{-5}$ Pa. Background of the reactor is controlled by mass spectroscopy.
8	*Set up the monomer flow rate by flow meter on the required value 3.8 sccm (corresponds to 29 sccm of* N_2 *flow meter)*. The water in the monomer bath is cooled to 15 °C permanently and mixed before deposition to reach homogeneous temperature in the whole volume. After stabilization of the monomer flow rate, it is possible to check monomer purity by mass spectroscopy and the pressure measured in the reactor chamber should be at value of 2.7 Pa.
9	*Plasma polymer deposition*. At first it is necessary to set up required generator power and generator regime: continual or pulse (in this regime also pulse duty cycle) by A3 controller. Then the plasma glow discharge for required deposition time is switched on. During glow discharge, it is possible to measure optical parameters of sample by in-situ spectroscopic ellipsometry and analyze the running processes in the plasma by mass spectroscopy measurements. After required time, the glow discharge is switched off and the pressure in the reactor chamber influenced by monomer flow is inspected, it should be near the value of 2.7 Pa. In conclusion monomer flow rate is switched off, and reactor chamber is evacuated for a while to reduce residual gases.
10	In the case of multi-layers preparation, after deposition of the first layer, the deposition parameters (power, regime, monomer flow rate, deposition time) have to be changed and the next layer is deposited on the previous layer but this time without activation by Ar plasma. In case of nanolayers preparation, where layer has to have resulting thickness under 100 nm, the shutter between bottom electrode with samples and upper electrode is used for 1 minute stabilization of plasma condition and to prevent the deposition on the substrate or sample. After stabilization, the shutter is moved off the plasma zone and the deposition of nanolayer on substrates or samples starts.
11	*Reduction of free radicals at argon atmosphere*. After plasma deposition, 10 sccm of argon

	gas is let into reactor by flow meter during the time of 1 hour. The argon gas purity can be checked by mass. After an hour, the argon gas is switched off, the reactor chamber is evacuated and samples are measured by spectroscopic ellipsometry to obtain their optical properties and thickness after deposition. Samples are kept in the reactor to the next day to reduce free radicals.

2.2 PLASMA DIAGNOSTICS

2.2.1 Mass spectroscopy

The mass spectra discussed in this work were measured by mass spectrometer HIDEN Analytical Company equipped with quadrupole mass analyzer and with Faraday and SCEM detectors measuring up to 500 amu. (atomic mass units) with maximum resolution 0.001 m/z. Spectra were measured up to 150 m/z with resolution 0.01 m/z by the regime SAMPLE PROCESS GAS during monomer deposition or up to 50 m/z during argon plasma measurement.

2.3 CHARACTERIZATION OF PLASMA POLYMER FILMS

2.3.1 Chemical composition

Fourier Transform Infrared Spectroscopy (FTIR)

Infrared measurements were carried out using a Nicolet Impact 400 Fourier transform infrared (FTIR) spectrophotometer. For the background noise reduction 256 scans were used. Measuring range was from 400 to 4000 cm^{-1} with a resolution of 0.96 cm^{-1}. The measuring space was flushed by flow of dry air (air from compressive distribution run through zeolit filter, which entrap most of the residual water vapor) at least 20 minutes before each measurement to reach defined atmosphere. Some samples were measured on the new type of FTIR device (Nicolet iS10, Thermo Scientific) with continual flow of dry air and with automatic function of atmosphere suppression and H_2O and CO_2 correction. The number of scans during measurements was set up to 256 with a resolution of 0.482 cm^{-1}. The thickness of thin layers analyzed by FTIR was in the range of 80 nm to 2 μm.

X-ray Photoelectron Spectroscopy (XPS)

The composition of elements (C, Si, O) in the surface region (top 6-8 nm) of the deposited layers was determined by XPS on an ADES 400 (VG Scientific U.K.) photoelectron spectrometer using Mg$K\alpha$ (1253.6 eV) photon beams at the normal emission angle and equipped with a twin anode X-ray source with the standard Al/Mg anodes and a rotable hemispherical energy analyzer. Atomic concentrations were determined from the C 1s Si 2p and O 1s lines assuming a model of semi-infinite solid which is homogeneous in composition [28]. The measurements were carried out in Institute of Physics of the Academy of Sciences of the Czech Republic.

Rutherford Backscattering Spectrometry (RBS)

The elemental composition in deep levels of plasma polymer thin film has also been studied by conventional and resonant RBS using the beam of 2.2 MeV He ions. Reflected particles were detected at 170° laboratory scattering angle. The hydrogen concentration was determined by Elastic Recoil Detection Analysis (ERDA, 2.7 MeV He ions and protons recoiled under the angle of 30°) methods using Van de Graaff generator with a linear electrostatic accelerator. The RBS spectra were evaluated by computer code GISA 3 and the ERDA ones by SIMNRA code both using cross-section values from SigmaBase. A systematic error of evaluated concentrations was up to 5 at. % [29, 30]. The measurements were carried out in Nuclear Physics Institute of the Academy of Sciences of the Czech Republic.

Contact Angle Measurement and Surface Energy Evaluation

The sessile drop method (tangent method) employing an OCA 10 goniometer (DataPhysics) with Software SCA 20 for Windows 9x/NT was used to measure the equilibrium contact angles.). Contact angle values were obtained as average from tangent measurements of both sides of the drop. Resulting contact angle values are an averages from results obtained from a set of 7 drops of each liquid. Standard deviation usually was about 1° and can be considered as good measurement [31, 32]. The surface free energy, as well as the dispersive and polar components of TVS thin films were evaluated using the approach of Owens-Wendt geometrical mean method and Wu harmonic mean method. The contact angle data of two different testing liquids are needed for the determination of surface free energy (and components) according to Owens-Wendt and Wu methods: distilled water − author Ström et al. and diiodomethane − author Janczuk et al.

2.3.2 Physical Properties

Ellipsometry

Ellipsometric spectra were measured by spectroscopic ellipsometer UVISEL® from Jobin-Yvon Company. Ellipsometer on the A3 apparatus is set up for measuring the polarized state of polarized light reflected respectively to polarized state of polarized light entering the system. Ellipsometer is phase-modulated, so parts of the ellipsometer (polarizer, modulator and analyzer) are fixed in the known positions. The samples were measured in the range of wavelengths from 250 to 830 nm with resolution 2 nm. The angle of measurement is for our samples in the range from 69.5 ° to 70.5 ° and had to be fitted before each measurement. A realistic model was used for fitting of measured data. With respect to mostly amorphous structure of the plasma polymers, Tauc-Lorentz model was chosen as model suitable for amorphous or almost amorphous materials.

X-ray reflectometry

The layer thicknesses, densities of layers and root mean square roughness [33] were measured in case of some samples using standard x-ray reflectometry through the use of high-resolution x-ray diffractometer with a conventional copper x-ray tube, parabolic multilayer mirror collimator and Ge 220 Bartels-type monochromator. The intensity was measured by a scintillation detector with a slit. The reflectivity was fitted by a model of two layers on a silicon substrate. First layer represents the polymer and the second is the thin silicon oxide layer between the substrate and the polymer layer. Gaussian model of interface roughness was used. The measurements were carried out in Department of Condensed Matter Physics in Masaryk University.

Atomic Force Microscopy (AFM)

Surface characterization of plasma polymer thin layers was carried out in non-contact mode by NTegra Prima/Aura (NT-MDT, Russia) scanning probe microscope (SPM) with optical viewing system (optical microscope). Microscope resolution is determined by used probe tip and radius of its curve. Usually the resolution between few nanometer and tenths of nanometers is reached. The single crystal silicon probe was used for our purpose. The scan area was 5 x 5 μm^2. Microscope is located on the active anti-vibration table, which inhibits vibrations from the surrounding in the range of 0.7 Hz – 1 kHz and is also equipped with passive isolation, which inhibits frequencies over 1 kHz. The Root means square (RMS) roughness was evaluated by the help of software.

Nanoindentation

The nanoindentation experiment was carried out on triboscope system from Hysitron Company, Minneapolis, USA, which is attached to an NTegra Prima Scanning Probe Microscope. During nanoindentation measurements, the Berkovich tip with a radius of curvature of about 150 nm and 50 nm were used for the analysis of thin films, multilayer films, gradient films and can be also be used for scratch study of thin films on silicon substrate. The main variable parameters for conventional test are the different loads (μN) and measurement time (s) of experiment. The load can be changed from 1 μN to 10 mN and experiment time from minimum 3 sec to minutes. The load/unload vs. displacement curve is obtained by indentation experiment. The mechanical properties (e.g. Young modulus, hardness) at a given contact depth of the indenter are calculated according to the Oliver-Pharr method [34].

3 RESULTS AND DISCUSSION

3.1 PLASMA POLYMERIZED TETRAVINYLSILANE FILMS

After determining stable deposition conditions in apparatus A3 for continual plasma regime, optimal set of single layers from tetravinylsilane monomer was chosen for deposition and characterization. Plasma polymer films of tetravinylsilane monomer (TVS, purity 97 %, Sigma-Aldrich) were deposited on polished silicon wafers (100, 0.8 × 10 × 10 mm^3, with impurity max. 6.9 – 8.9 × 10^{17} $at.cm^{-3}$, Terosil Co., Czech Republic) by plasma-enhanced chemical vapor deposition (PE CVD). The substrates were pretreated with argon plasma (10 sccm, 5.0 Pa, 5 W, continual mode) for 10 min to improve the film adhesion. Plasma-polymerized tetravinylsilane (pp-TVS) films were deposited at a mass flow rate of 3.8 sccm (which corresponds to $p_{TVS} \approx 3.0$ Pa) and the RF power in a range of 10 – 70 W on 6 identical silicon wafers (substrates). Each of 6 samples from one set deposited at the same RF power (marked from "a" to "f") was characterized by different method. Uniform plasma polymer films were deposited with a film thickness of about 1 μm. Deposition conditions (power, pressure, deposition time) are given in Table 2.

Table 2: Deposition conditions for single pp-TVS films

Sample	RF power P [W]	deposition pressure p_{dep} [Pa]	deposition time t_{dep} [s]
3065 $_{(a-f)}$	10	1.6	420
3066 $_{(a-f)}$	20	1.4	360
3067 $_{(a-f)}$	25	1.3	390
3068 $_{(a-f)}$	50	1.2	361
3069 $_{(a-f)}$	70	1.0	347

3.1.1 Mass spectroscopy

The set of measurements during plasma depositions of tetravinylsilane with different RF powers (10 – 70 W) were carried out by mass spectroscope. The influence of the RF power on the monomer fragmentation is summarized in the Figure 3. The graph is in the logarithmic scale for better general comparison, where each y-axis is in the range of 3.25 × 10^{-11} – 5 × 10^{-8} Torr. All spectra were measured at a monomer mass flow rate F_{TVS} = 3.8 sccm, which corresponds to the pressure in the reactor chamber $p_{TVS} \approx 3$ Pa without plasma discharge. Mass spectrum of tetravinylsilane monomer without discharge is also included in the Figure 3 for comparison. It is evident, that with increasing of the RF power, enhanced monomer fragmentation occurred and so fragments with higher mass number decreased and contrary fragments with smaller mass number increased. Significant fragments were identified and described in the Table 3. During lower RF powers, contents of higher molecular fragments increases as well as content of their derivatives, which correspond to TVS molecule with one, two or three eliminated vinyl groups (derivatives have eliminated one or more of hydrogen atoms in addition). This trend

hints that the preferential bond, which is broken in the monomer, is the bond between silicon and vinyl group. During higher RF powers, these separated vinyl groups and other higher particles are fragmented to smaller particles, eventually up to atomic level. The growth of these smaller particles can be observed. Especially molecular hydrogen with mass number m/z = 2, which is created by recombination of atomic hydrogen originating in plasma discharge by elimination from monomer molecule, increases with increasing RF power.

Table 3: Particles identified by mass spectroscopy

m/z	Identification of fragments by MS
2	H_2
15	CH_3^+
24	$C^{\bullet}\equiv C^+$
25	$HC\equiv C^+$
26	$HC^{\bullet}=CH^+$
27	$H_2C=CH^+$
28	$H_2C^{\bullet}-CH_2^+$
29	$H_3C-CH_2^+$
31	SiH_3^+
39	$H_2C=C=CH^+$
43	$H_3C-CH_2-CH_2^+$ $HSi^+=CH_2$
55	$C_2H_3Si^+$
57	$C_2H_5Si^+$
67	$C_3H_3Si^+$
83	$C_4H_7Si^+$
95	$C_5H_7Si^+$
109	$C_6H_9Si^+$

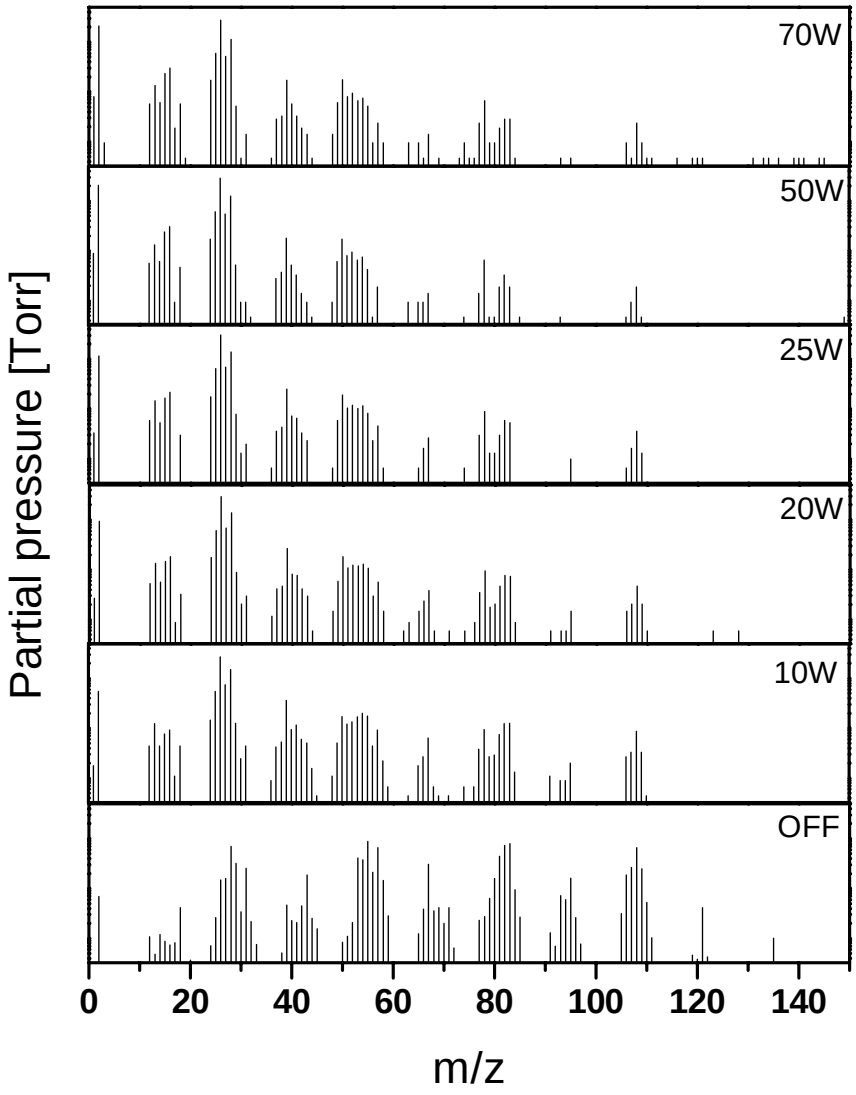

Figure 3: Comparison of mass spectra of plasma polymer layers deposited with different RF powers, in logarithmic scale

3.1.2 Spectroscopic ellipsometry

Single layer films deposited at a power set on 10, 20, 25, 50, and 70 W were characterized by spectroscopic ellipsometry to evaluate not only their thickness but the dispersion dependences of optical constants (refractive index and extinction coefficient) in the wavelength range of 250 – 830 nm.

The dispersion curves (see Figure 4) evaluated from spectroscopic ellipsometry were well separated according to the power used and the pp-TVS films were relatively well transparent. The dispersion dependence for the refractive index moved to higher values with enhanced power and the refractive index at a wavelength of 633 nm increased from 1.69 (10 W) to 2.08 (70 W). This behavior corresponds to an increased density of polarizable species in a-SiC:H alloy due to

higher cross-linking of plasma polymer with enhanced power. Extinction coefficient increased towards infra-red area with increased RF power used during deposition.

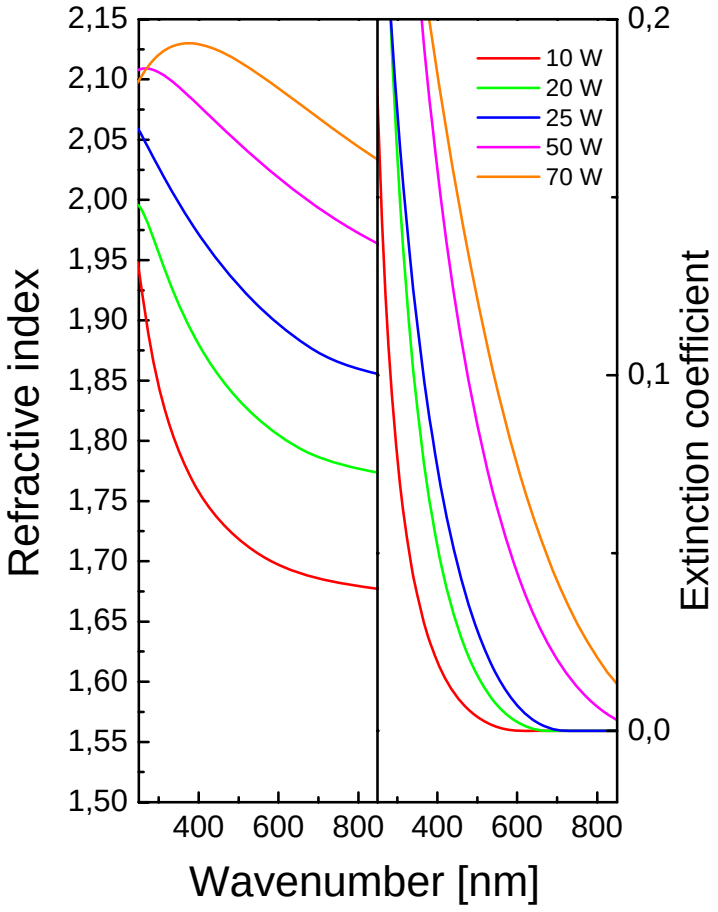

Figure 4: Dispersion curves for the refractive index and extinction coefficient of single layer films deposited at different RF powers

The deposition time for each sample of single layer was chosen to reach film thickness of 1 μm, suitable for next analysis and characterizations. Film thickness of plasma polymerized single layers prepared at different RF powers, measured after deposition and evaluated by ellipsometer was 1004 nm (10 W), 1010 nm (20 W), 1124 nm (25 W), 1030 nm (50 W) and 1010 nm (70 W).

Deposition rate (nm/s) was evaluated from resulting thickness of prepared pp-TVS layer measured by ellipsometer after deposition and from deposition time. At higher RF power (over 25 W) deposition rate is almost constant and saturation occurs. Also another monomers exhibited identical behavior [2]. The deposition rate was ranging from 140 to 173 nm/min as a function of the deposition conditions.

Dependence of the energy gap (eV) on the RF power for set of single layer films can be seen in the Figure 5. Energy gap is evaluated from ellipsometer measurements and its value influences the extinction coefficient. Spectra were measured immediately after deposition. The layer prepared at 10 W has energy gap

of 2.01 eV after deposition and belongs to semiconductors material, while the layer prepared at 70 W has energy gap of 1.16 eV, so with increasing RF power, the energy gap decreases slowly and material is more conductive.

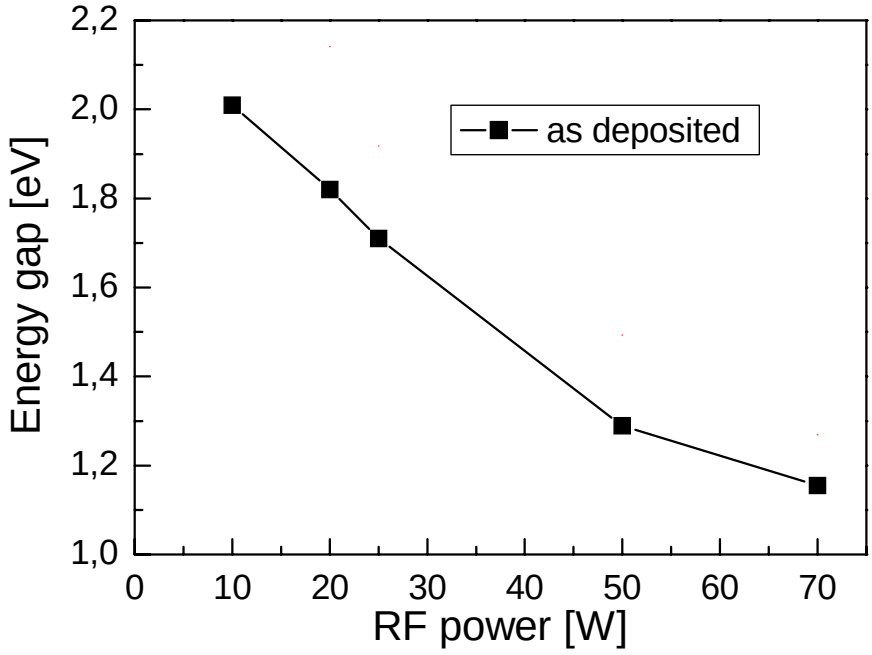

Figure 5: Dependence of the energy gap (eV) on the RF power (W) for set of single layer films measured after deposition

3.1.3 Fourier Transform Infrared Spectroscopy (FTIR)

In the Figure 6, compared FTIR spectra of plasma polymerized TVS layers prepared with different RF powers from 10 W to 70 W can be seen. Characteristic function groups were assigned to absorption bands and are summarized in the Table 4. The first marked peak recorded in the spectra from the highest wavenumbers is absorption band at 3600 – 3200 cm^{-1}, assigned to –OH groups (marked as A). With regard to absence of oxygen in monomer molecule, this absorption band would not occur in the spectra. If the FTIR spectrum is measured immediately after deposition, this absorption band is very weak or is missing completely, as was already discussed in the Ref. [35]. Similar situation is with absorption bands assigned to C=O stretching vibration at wavenumber 1714 cm^{-1} (marked as E) and absorption bands assigned to Si-O-C, Si-O-Si stretching vibrations at wavenumber 1100 – 1000 cm^{-1} (marked as J). All these absorption bands are more intensive after exposition to the atmosphere. Yet it can be seen, that these absorption bands are strongest in the spectra of layers prepared at lower RF powers. Mass spectrometry measurements suggested that this kind of polymer is lower crosslinked. Due to this, the atmospheric oxygen is easily infiltrated into layers prepared at lower RF powers and

discussed absorption bands connected with oxygen are strongest in this type of layers. Their intensity decreases with increasing power, so layers prepared at higher RF powers are more stable and resistant to atmospheric degradation.

Another absorption band, which is very weak, can be observed at 3312 cm^{-1} and is assigned to second harmonic vibration C=C stretching in vinyl (marked as B). Its fundamental vibration has wavenumber at 1591 cm^{-1} (marked as F). Another important absorption bands which represents vinyl groups and are presented in prepared plasma polymerized layers are -CH_2 deformation in vinyl at 1412 cm^{-1} (marked as H) and =CH or =CH_2 wagging in vinyl at 1015 cm^{-1} (marked as K) and 959 cm^{-1} (marked as L), respectively. Intensities of these vinyl vibrations increased with decreasing RF power. This trend agrees well with measurements of mass spectroscopy which confirm molecule TVS ionization and dissociation to smaller fragments at higher RF powers and so highest content of vinyl groups during depositions with lower RF powers.

The group of absorption band at wavenumber 3000 – 2800 cm^{-1}, assigned to CH_2 and CH_3 stretching vibrations (marked as C), decreased its intensity with increasing RF power. The absorption band at 1461 cm^{-1} is also associated with function group CH_2 (marked as G) and it seems that its intensity decreased slightly with decreasing RF power and during lower RF power, this scissoring vibration is partially overlapped by vibration of vinyl group at 1412 cm^{-1}.

Another groups presented in spectra and containing silicon, marked as D, I, M and N, are assigned to Si-H stretching vibration at 2122 cm^{-1}, CH_2 wagging vibration in Si-CH_2-R at 1255 cm^{-1}, Si-H bending vibration at 845 cm^{-1} and Si-C stretching vibration at 732 cm^{-1}, respectively. Their absorption band intensity decreased with increasing RF power. It suggested that C/Si ratio increased with increasing power and material is formed more by carbon at higher RF powers. This trend is confirmed also by ellipsometry and mass spectroscopy measurements. The intensity of relatively sharp absorption band assigned to CH_2 wagging vibration in Si-CH_2-R increased with decreasing RF power, which also suggested lower monomer fragmentation at lower RF powers and by that preservation of bonds Si-CH_2 in plasma polymer. The group of absorption bands between wavenumbers 1100cm^{-1} – 920 cm^{-1} was discussed above and as can be seen, the intensity of Si-O-C stretching vibration, Si-O-Si stretching vibration and two sharp absorption bands assigned to =CH and =CH_2 wagging vibrations in vinyl, increased with decreasing RF power. It is caused by lower crosslinking of plasma polymer and so easier penetrating of atmospheric oxygen to prepared layer and by lower fragmentation of monomer at lower RF powers and so higher content of vinyl groups in the plasma polymer.

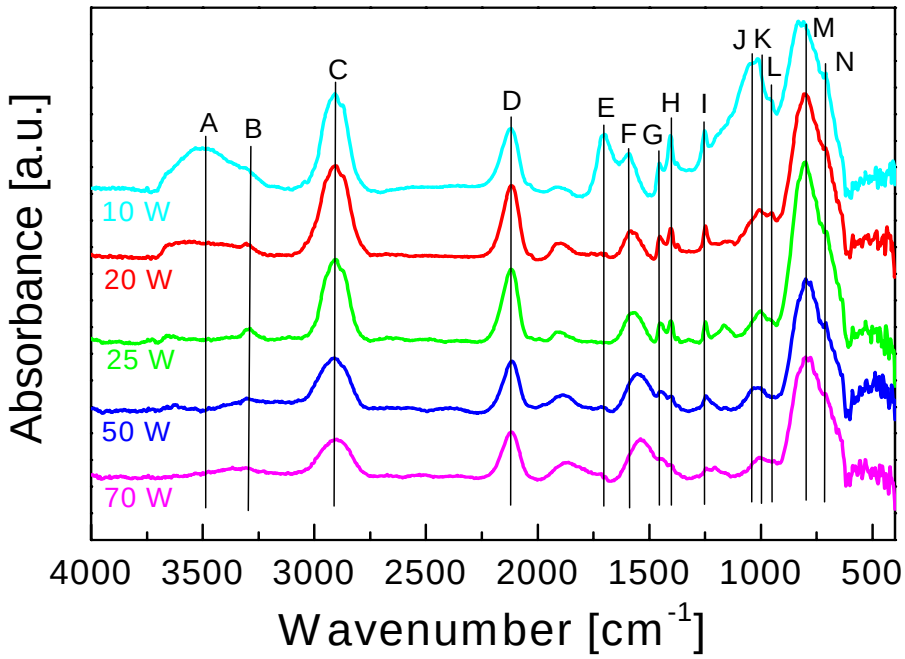

Figure 6: FTIR spectra of pp-TVS layers prepared at different RF powers

Table 4: Assignment of function groups to the absorption bands of pp-TVS

Absorption band	Wave number (cm^{-1})	Assignment
A	3650−3200	O−H stretching
B	3312	C=C stretching in vinyl
C	3000−2800	CH_2, CH_3 stretching
D	2122	Si−H stretching
E	1714	C=O stretching
F	1591	C=C stretching in vinyl
G	1461	CH_2 scissoring
H	1412	CH_2 deformation in vinyl
I	1255	CH_2 wagging in $Si-CH_2-R$
J	1100-1000	Si−O−C, Si−O−Si stretching
K	1015	=CH wagging in vinyl
L	959	$=CH_2$ wagging in vinyl
M	845	Si−H bending
N	732	Si−C stretching

3.1.4 Rutherford Backscattering Spectrometry (RBS) and Elastic Recoil Detection Analysis (ERDA), X-ray photoelectron spectroscopy (XPS)

The results from measurements of pp-TVS layers prepared at different RF powers, measured by RBS and ERDA methods, can be seen in the Figure 7. These measurements were carried out approximately one month after sample depositions so the results are influenced by atmospheric degradation and by oxygen permeation into the layers. In the Figure 7 you can see atomic concentration [at %] of hydrogen, carbon, silicon and oxygen of pp-layers from TVS depending on the RF power. RBS measurements provide information from depth levels of sample.

The hydrogen concentration, which was measured by ERDA method, generally decreased with increasing RF power, from 64 % for layers prepared at 10 W to 40 % for layers prepared at 70 W. Concentration of carbon, measured by RBS, increased with increasing RF power, from 25 % for layers prepared at 10 W to 53 % for layers prepared at 70 W. Oxygen concentration, according RBS measurements, generally decreased slightly with increasing RF power, from 5 % for layers prepared at 10 W to almost 0 % for layers prepared at 70 W. Silicon concentration measured by RBS seems to increases with increasing power, from 5 % for 10 W to 7 % for 70 W. These negligible changes can be considered as the measurements error. Measurement error of these methods in the case of our samples is estimated at 5 at. %. Also in comparison with FTIR measurements, where the absorption bands assigned to groups containing silicon rather decreased with increasing power, at an expense of carbon increasing at higher RF powers. Silicon grow is recorded especially in layers prepared at 25 W, which could be connected only with slightly increasing of Si-H absorption band measured by FTIR in the case of layer prepared at 25 W. Marked changes in atomic concentration, especially in the case of hydrogen and carbon, were also recorded in layers prepared at 25 W.

Element ratios were calculated from RBS measurements and compared depending on RF power. With increasing RF power, element ratio C/Si generally increases from 4.6 to 7.4 for 10 W and 70 W respectively. Ratio C/Si expresses the change in organic-inorganic character of material. Material gains more organic character with increasing RF power in the depth level of samples. Predisposition of pp-layers to oxidation can be express by element ratio O/Si, which slightly decreases with increasing RF power from 1 to 0 for 10 W and 70 W respectively. Samples prepared at lower RF powers are more subject to atmospheric degradation. Element ratios O/C seems to be generally constant at all course of RF powers (from 0.2 to 0.0 for 10 and 70 W respectively).

The comparison of atomic concentrations depending on RF power, received from XPS and RBS measurements, can be seen in the Figure 8. XPS measurements were carried out 10 months after deposition and provide information about atomic concentration from top levels of sample (up to 6 nm). RBS measurements were carried out year after deposition (as was already mentioned). In the Figure 8 you can see RBS results measured only in the zone of thickness from surface to 0.2 μm, for better comparison with XPS measurement. As can be seen, carbon concentration

increased with increasing RF power in case of XPS measurement as well as RBS measurement. XPS measurements show higher content of carbon on surface in case of pp-layers prepared at lower effective powers. Oxygen concentration decreased with increasing RF power, in case of XPS measurement less intensively than in case of RBS measurement. It is evident that post-deposition degradation on the atmosphere is intensive especially on the surface of pp-layers and the content of oxygen decreased with thickness. The results also confirmed the higher post-deposition stability of samples prepared at higher RF powers. Silicon concentration is constant in case of the XPS measurements but not in case of the RBS measurement. These changes can be connected with higher content of Si-H groups in layers prepared at 25 W, as was proven by FTIR measurements but also with relativity of atomic concentration evaluation and so connected changes in carbon and oxygen concentrations at 25 W. Generally, silicon concentration can be considered as constant.

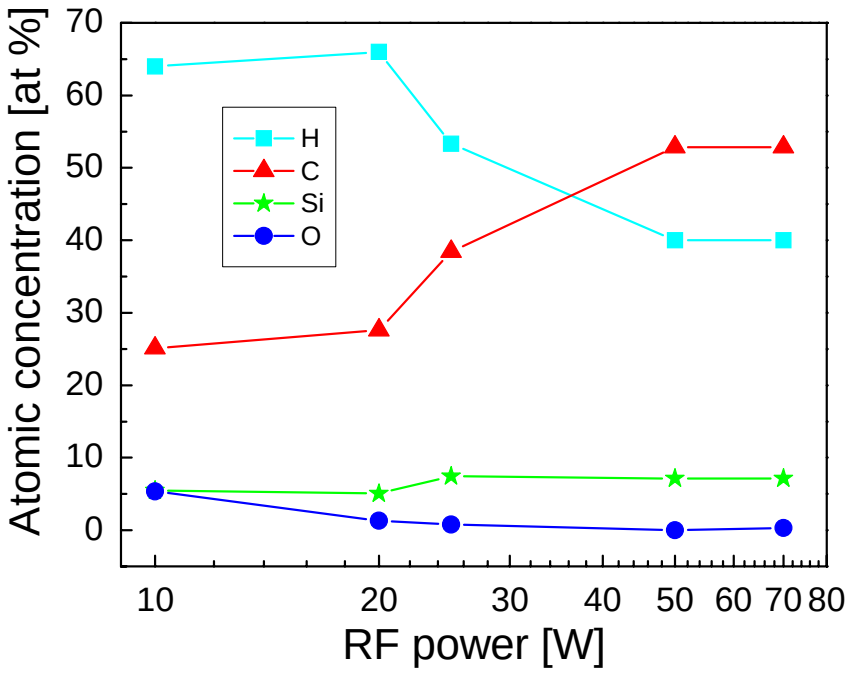

Figure 7: Dependence of the atomic concentration of pp-TVS layers on the RF power measured by RBS and ERDA

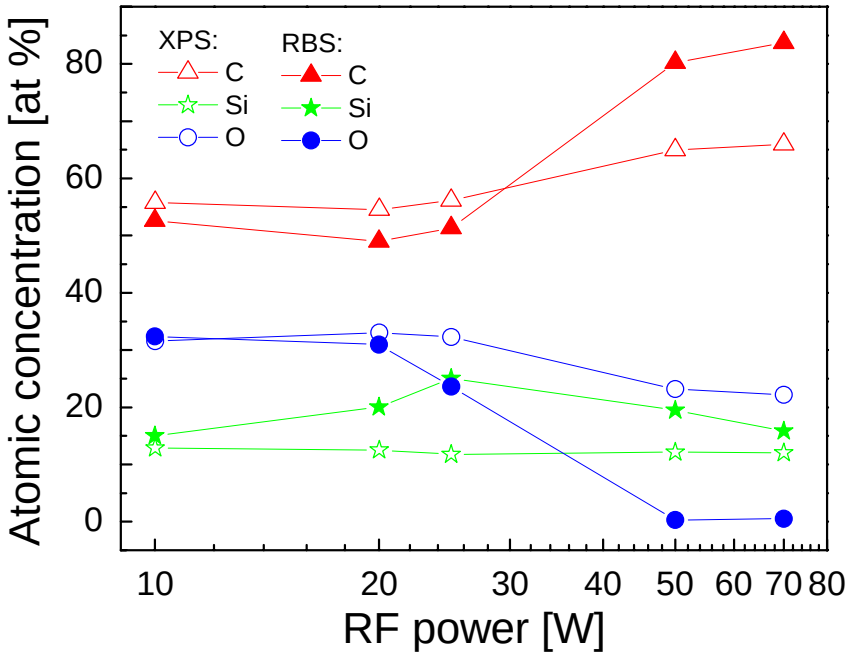

Figure 8: Comparison of atomic concentrations measured by XPS and RBS methods, depending on the RF power

3.1.5 Atomic Force Microscopy (AFM)

Surface morphology and Root Mean Square (RMS) of pp-thin films from tetravinylsilane was pursued by AFM microscopy. The surface of pp-thin films is indented and mainly formed by rounded shapes with height up to tents of nanometers. Peaks on surface of layers prepared at lower RF powers are more sharp and smaller (about 40 nm) than peaks on surface of layers prepared at higher RF powers, which are rather round and higher (up to 80 nm). Pp-TVS layers deposited at lower RF powers have smaller roughness than thin layers prepared at higher RF powers.

The root means square (RMS) roughness was evaluated by the help of software. In the Figure 9 dependence of the RMS roughness (nm) on the RF power (W) of pp-TVS layers deposited with thickness of about 1 μm can be seen. Evaluated RMS roughness increased with enhanced power from 3.4 nm for pp-layers prepared at 10 W to 22 nm for pp-layers prepared at 70 W. Increasing of RMS roughness with enhanced power of pp-layers from TVS prepared in tubular chamber apparatus was also noticed and discussed in the Reference [36].

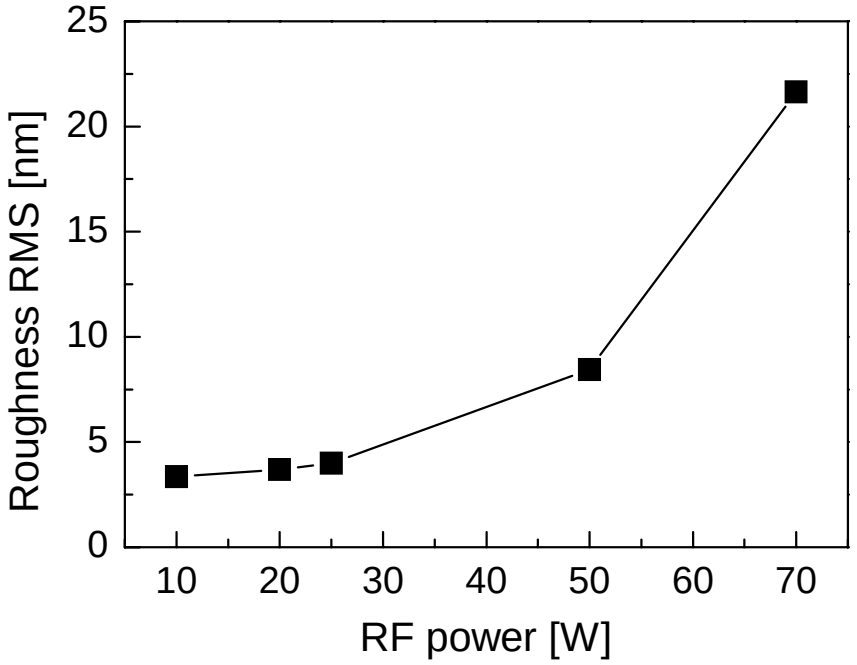

Figure 9: Dependence of the RMS roughness of the pp-layers from TVS on the RF power

3.1.6 Nanoindentation

Mechanical properties of plasma polymers are important parameters regarding to their usage as interphase in the composite material. Mechanical properties of pp-TVS layers prepared at different RF powers were determinate by nanoindentation measurements. Load-displacement curves during penetrating of diamond tip to the depth up to 100 nm were measured. Depth of displacement was up to 10 % of film thickness to eliminate the influence of substrate. From load-displacement curves, the mechanical properties like Young modulus and hardness were evaluated.

In the Figure 10, dependence of the mechanical properties on the RF power can be seen. Hardness and Young modulus increase with increasing RF power. Change of the mechanical properties is connected with structure of prepared material. Layers prepared at higher RF powers have higher contents of carbon than silicon and are more crosslinked, which leads to higher values of mechanical properties. Growth of the Young modulus and hardness with enhanced RF power was also noticed at pp-TVS layers prepared in tubular chamber and discussed in the Reference [36].

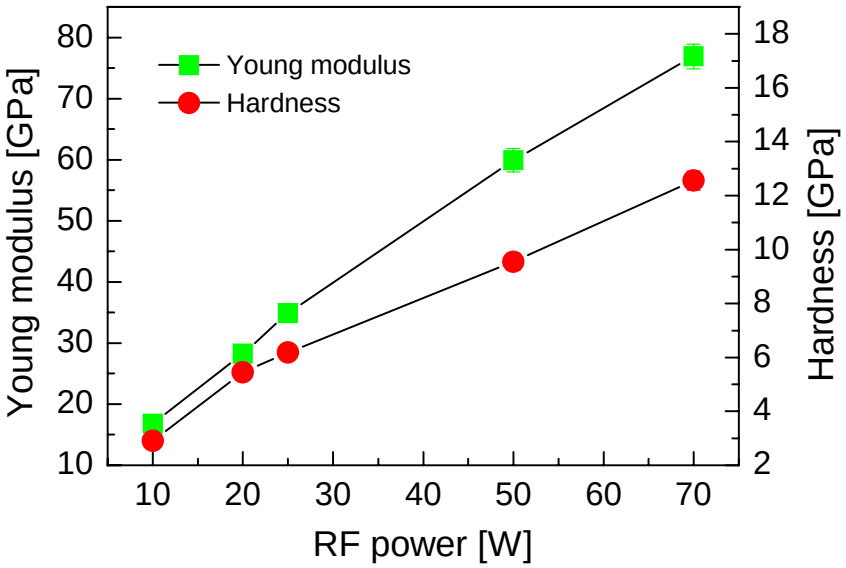

Figure 10: Young modulus and Hardness of pp-TVS layers depending on RF power

3.1.7 Contact angle and Surface free energy

Sessile drop measurements were employed to measure equilibrium contact angles of the pp-films and evaluated the surface free energy by Owens-Wendt (O-W) and Wu methods. Measured contact angles (in deg.) of the probe liquids were changed according to various magnitudes of the input RF power (W). In the Figure 11 the dependence of the contact angle (in deg.) of two probe liquids (water and diiodomethane) on the RF power (W) can be seen. The contact angle of water (bipolar probe liquid) slightly decreases with increasing RF power except 70 W. Also trend of decreasing contact angle of diiodomethane (apolar probe liquid) with the magnitude of the input RF power can be seen.

In the Figure 12, there can be seen calculated total surface free energy for set of samples, by O-W geometric mean and Wu harmonic mean methods, depending on the RF power. Total surface free energy is sum of dispersion γ^{d} and polar γ^{p} components. Values obtained by Wu method are not exactly equal to the values obtained by O-W method. It is caused by different γ^{d} and γ^{p} values of probe liquid diiodomethane. Total surface free energy (of both methods) and wettability increase with increasing RF power. It means that pp-TVS thin films prepared at lower RF powers are less hydrophilic than films prepared at higher RF powers. This trend does not correspond with results from FTIR spectroscopy, which suggested the presence of OH groups (strong polar) and C=O groups (middle polar) in the pp-TVS layers prepared at lower RF powers. The presence of these hydrophilic groups should cause the higher values of surface free energy. Contradiction is probably caused by contact angle measurements immediately after deposition, which implies less atmospheric degradation and oxygen incorporation into surface of layers, while

FTIR spectra were measured two weeks after deposition, so atmospheric degradation and oxygen incorporation occurred especially in pp-layers prepared at lower RF powers.

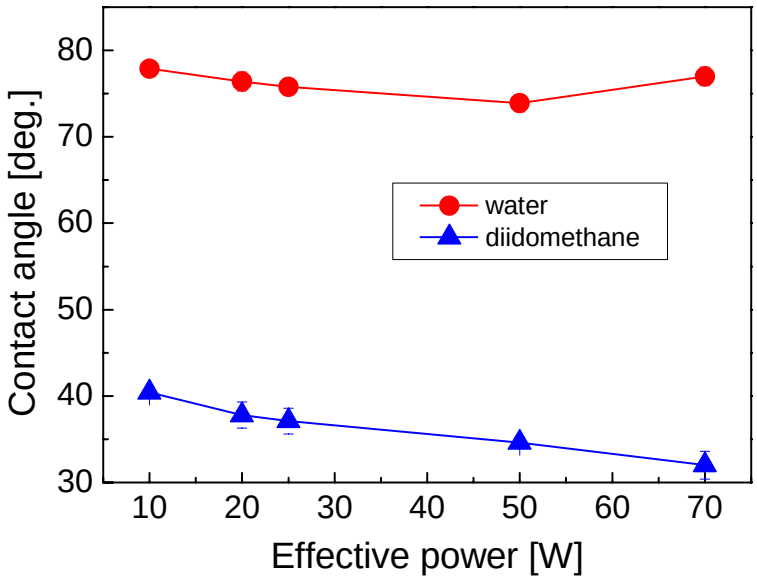

Figure 11: Dependence of the contact angle of all testing liquids on the magnitude of the input RF power

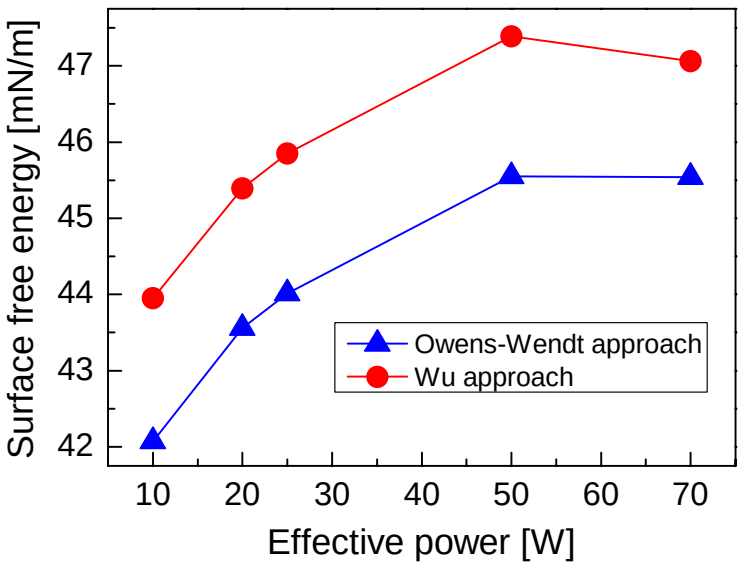

Figure 12: Dependence of surface free energy evaluated by Owens-Wendt and Wu approach on the magnitude of the input RF power

3.2 UV TREATMENT OF PP-TVS FILMS

Plasma-polymerized tetravinylsilane (pp-TVS) films were deposited on silicon wafers at RF power of 10 W in continual regime. Two batches, each of six samples, with a film thickness of 0.1 μm and 0.5 μm, respectively, were deposited using the same deposition conditions. The as-deposited films were subjected to UV irradiation at ambient conditions for different times ranging from 10 to 1000 min. Modifications of the chemical and physical properties of the irradiated films were investigated in comparison with those of the reference sample (as-deposited film).

The irradiated films were immediately characterized by FTIR and spectroscopic ellipsometry and again subsequently over the next 134 days (30 min, 1 h, 4, 24 h, 4 days, 15, 86, 134 days). FTIR spectra of 0.5-μm films as-irradiated by UV light are compared with the reference film (as deposited, sample F) in Figure 13. Differences in absorption bands are clearly evident for increasing UV exposition time. A descending concentration of CH_x (2780-3034 cm^{-1}) and SiH (2055-2240 cm^{-1}) species is apparent at prolonged UV exposition time, with the absorption bands quite missing at a UV exposition time of 1000 min, suggesting elimination of hydrogen from the irradiated material. The hydrogen reduction in a-SiOC:H (hydrogenated amorphous carbon-silicon oxide) alloys was observed by Verdonck *et al.* using the PECVD process combined with UV irradiation [37]. However, a significant increase of hydroxyl (3204-3630 cm^{-1}), carbonyl (1685-1842 cm^{-1}), and Si–O–C (990-1238 cm^{-1}) species can be found in spectra at prolonged UV irradiation times up to 333 min (sample D), but this is followed by an abruptly increased concentration of Si–O–C species with a decrease of hydroxyl and missed carbonyl groups at 1000 min (sample E). FTIR spectra (Figure 13) indicated changes in chemical structure of UV-light modified films. Oxygen atoms were incorporated into the plasma polymer forming Si–O–C, OH, and C=O species due to the oxidation effect under UV irradiation.

Similar trends were found for some as-irradiated and the as-deposited samples stored at room temperature (about 22^{o}C, 30% humidity) and observed over 134 days to investigate aging effects. The greatest change in infrared spectra was observed for the reference film (sample F). The differences in FTIR spectra suggest that oxygen is partly incorporated into the plasma polymer network forming Si–O–C bonding species at the expense of Si–C species, and partly forming side groups (OH, C=O) at the expense of CH_x and SiH species. Longer UV exposition resulted in a smaller aging effect. There was no apparent difference among spectra of 1000-min-UV-irradiated film observed over 134 days. FTIR spectra of the thinner set of films (0.1 μm) corresponded to those with a film thickness of 0.5 μm, indicating an approximately homogeneous UV-light modification across a thicker film.

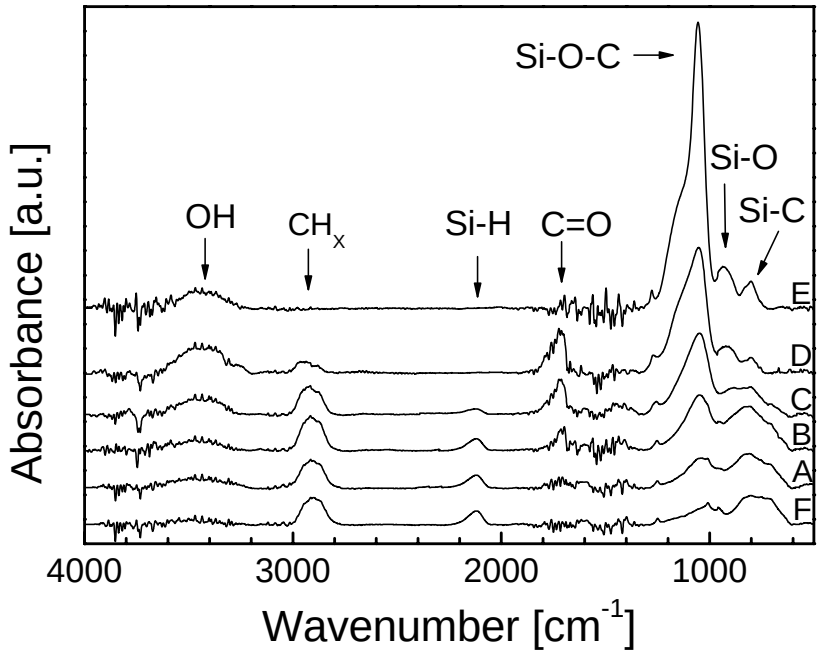

Figure 13: FTIR spectra of 0.5-μm films irradiated by UV light (10 min – sample A; 33 min – B; 100 min – C; 333 min – D; 1000 min – E) compared with the reference sample (as-deposited, sample F)

Analyses of XPS spectra enabled us to determine the elemental composition of pp-TVS films with a film thickness of 0.5 μm after 134 days of aging. Atomic concentrations of carbon, silicon, and oxygen dependent on UV exposition time are given in Figure 14. The carbon concentration decreased from 66 at.% (reference, sample F) to only 28 at.% for the film UV-irradiated for 1000 min, while oxygen and silicon concentrations increased significantly. The increase of silicon atoms in the pp-TVS films with prolonged UV irradiation is only illusory, as we cannot conceive of any source for additional silicon atoms that could contaminate the films. Further, a release of volatile products containing silicon atoms during UV irradiation of films is not probable and, thus, invariable silicon content for all pp-TVS films is a good assumption. Therefore, the C/Si and O/Si rates (Figure 14) give an accurate idea of changes in the chemical composition of pp-TVS films under UV irradiation.

The highest O/Si ratio was found for the aged reference sample corresponding to the highest aging effect confirmed by FTIR spectra (Figure 13). Oxidation of pp-TVS films resulted in the formation of carbonyl, hydroxyl groups, and modification of the plasma polymer network forming Si–O–C bonding species. The plasma polymer network is formed by Si–O–C bonding species instead of Si–C bonds – i.e., the less strong Si–C bond (290 kJ/mol) is substituted by stronger Si–O (369 kJ/mol) and C–O (351 kJ/mol) bonds [38].

The C/Si ratio decreased rapidly with prolonged UV exposition (Figure 14) and confirmed a significant reduction of carbon in UV-irradiated samples. It is known that UV irradiation can decompose conventional polymer materials such as polyurethane [39] or polyethylene [40], resulting in carbon reduction. Gas chromatography was used to analyze volatile organics produced during UV irradiation of polyethylene; the organics were determined as methane, ethene, ethane, and propane [40]. Such organics can be produced by scission of plasma polymer chains by UV photons.

Analyses of RBS and ERDA spectra confirmed that the bulk elemental composition of the films corresponded to the surface composition obtained from XPS spectra (Figure 14) and revealed elimination of hydrogen from the UV-irradiated material, indicated by FTIR spectra (Figure 13). A hydrogen concentration of about 45 at.% was determined for samples F, A, and B, but decreased with prolonged UV exposition to 15 at.% for sample E (1000 min UV exposition). The RBS/ERDA results indicate that all the films were approximately homogeneous except for sample D, which exhibited a small gradient profile with a slightly increasing carbon concentration from the film surface into the bulk.

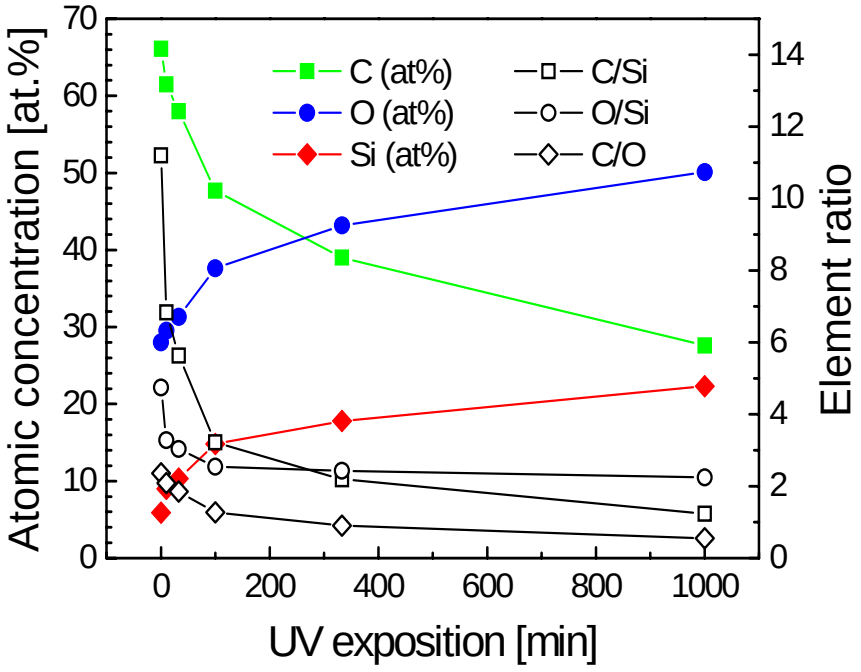

Figure 14: Elemental composition (carbon, oxygen, silicon) measured by XPS and element ratio of pp-TVS films as a function of UV exposition time.

Optical characterization of the films requires not only an appropriate parameterization of the material optical constants but also a realistic model of the sample structure. Our models consisted of a semi-infinite substrate (crystalline

silicon together with a silicon dioxide layer), a plasma polymer layer, and a surface overlayer (OL) corresponding to the surface roughness of the film [41]. The overlayer was modeled as the effective medium [42] with a fixed ratio (50%) of the plasma polymer and air. Ellipsometric data obtained for uncoated silicon wafers enabled us to evaluate the thickness of the silicon dioxide layer at the surface of the wafer; the value was 3.1 nm. This parameter was fixed for all the sample models in the form Si-SiO_2/layer/OL. The resulting dispersion curves for the refractive index and the extinction coefficient of all the samples (as-irradiated and as-deposited samples A – F) are shown in Figure 15. The refractive index (extinction coefficient) significantly decreased from 1.67 (0.124) for sample F to 1.39 (0.006) for sample E at a wavelength of 633 nm (250 nm) with prolonged UV exposition time. The decrease of the refractive index can be explained by an increased degree of oxidation of the plasma polymer network transformed from Si–C to Si–O–C bonding species due to the increased band gap of a-SiOC:H alloy.

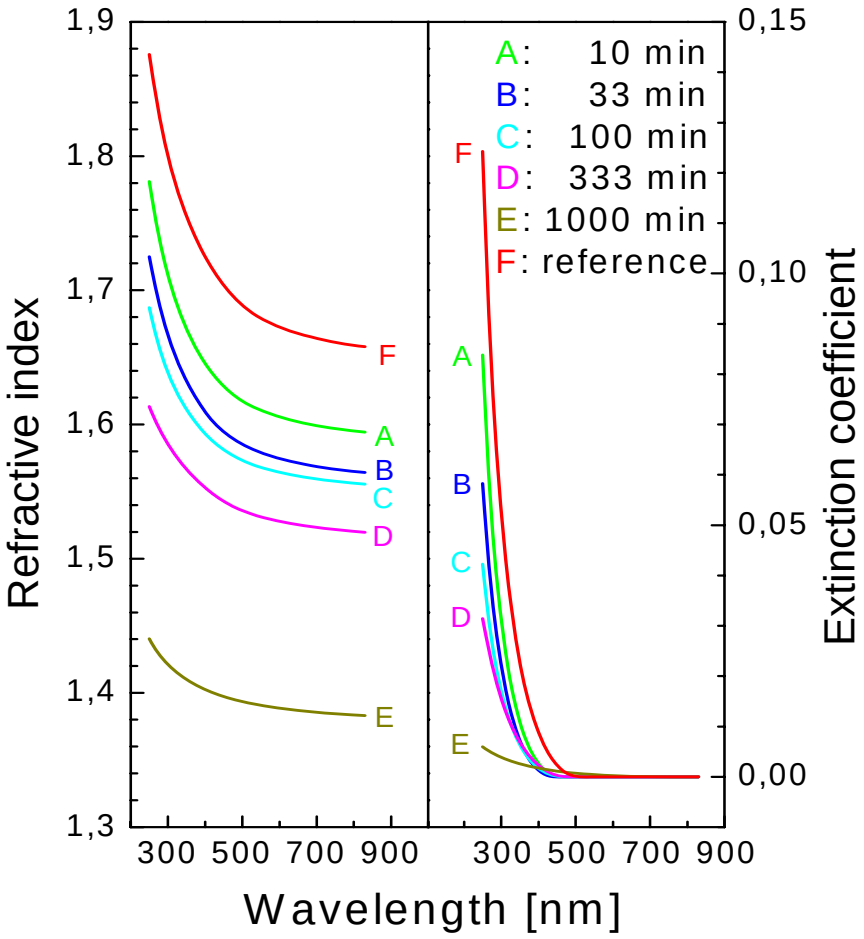

Figure 15: Dispersion curves of the refractive index and extinction coefficient for the reference (as-deposited film) and UV-irradiated samples.

Spectroscopic ellipsometry revealed a reduction of the film thickness after 1000 min of UV exposition, as shown in Table 5 for a batch of 0.5-μm films and Table 6 for a batch of 0.1-μm films. The film thickness of sample E was half of that of the reference sample F. A mass reduction of high-density polyethylene films treated with UV light was monitored with a quartz crystal microbalance [43]. Thus, the researchers were able to analyze a decrease of the film thickness due to UV-induced chain scission and bond breakage producing volatile organics. The surface roughness of the polyethylene films increased as a result of the UV-ozone treatment because of the etching effect of the ozone. However, the RMS roughness of pp-TVS films decreased after 100 min of UV irradiation (Table 5), as no ozone was produced during our UV treatments (the wavelength threshold for ozone production is 181 nm).

UV-induced cross-linking of plasma polymer together with a stronger polymer network (Si–O–C) and the reduction of the film thickness could modify the mechanical properties and density of the material. For this reason, nanoindentation measurements were used to investigate selected mechanical properties (Young's modulus and hardness) of pp-TVS films after 134 days. An increase of the Young's modulus by 21% and hardness by 24% compared with the reference sample was found only for the film UV-irradiated for 1000 min (Table 5).

X-ray reflectivity enabled us to determine the density of the plasma polymer, with a growth of 25% found only for sample E (1000 min UV exposition) (Table 6). The X-ray reflectivity was fitted by a model of two layers on a silicon substrate. The first layer represents the polymer and the second is the silicon oxide layer at the surface of the silicon substrate. The standard Gaussian model of interface roughness was used. The fitted parameters were the thickness and density of the layers and the root mean square roughness of the interface. The film thickness corresponded well to that determined by spectroscopic ellipsometry (Table 6). Sample D could not be analyzed due to the gradient density of the polymer film, which agrees with the RBS/ERDA results. The increased density of sample E pushed the refractive index to slightly higher values in accordance with the Clausius-Mossotti relationship [44].

Table 5: Comparison of film thickness, surface and mechanical properties of films exposed to UV irradiation

Sample	UV exposition [min]	Film thickness [nm]	RMS roughness [nm]	Young's modulus [GPa]	Hardness [GPa]
F	0 (reference)	463 ± 46	0.41 ± 0.03	11.7 ± 0.5	0.82 ± 0.05
A	10	532 ± 53	0.41 ± 0.01	10.0 ± 0.5	0.80 ± 0.04
B	33	593 ± 59	0.41 ± 0.01	11.1 ± 0.6	0.91 ± 0.05
C	100	560 ± 56	0.38 ± 0.03	10.6 ± 0.8	0.75 ± 0.07
D	333	464 ± 46	0.21 ± 0.04	10.2 ± 0.2	0.72 ± 0.02
E	1000	228 ± 23	0.12 ± 0.01	14.1 ± 0.4	1.02 ± 0.01

Table 6: Comparison of film thickness and density of films exposed to UV irradiation

Sample	UV exposition [min]	Film thickness by ellipsometry [nm]	Film thickness by reflectometry [nm]	Density [g/cm^3]
F	0 (reference)	101 ± 10	114 ± 1	1.6 ± 0.1
A	10	112 ± 11	113 ± 1	1.6 ± 0.1
B	33	108 ± 11	111 ± 1	1.6 ± 0.1
C	100	110 ± 11	110 ± 1	1.5 ± 0.1
D	333	76 ± 8	N/A	N/A
E	1000	58 ± 6	60 ± 2	2.0 ± 0.1

Modified surface chemistry of UV-irradiated films could influence wettability. Contact angle measurements of distilled water and methylene iodide were applied to evaluate the surface free energy of the pp-TVS films after 134 days. The total surface free energy together with the dispersive and polar components was determined using the Wu harmonic mean method and can be seen in Figure 16. The Owens-Wendt approach (geometric mean method) gave similar values for the surface free energy reduced by approximately 2 mJ/m^2. The dispersion component was the same for all the films; however, the polar component slightly increased with prolonged UV exposition time from 24 to 29 mJ/m^2 at 333 min and then dropped to 8 mJ/m^2 at 1000 min of UV exposition. This behavior can be well correlated with the concentration of polar hydroxyl and carbonyl groups in the plasma polymer (Figure 13).

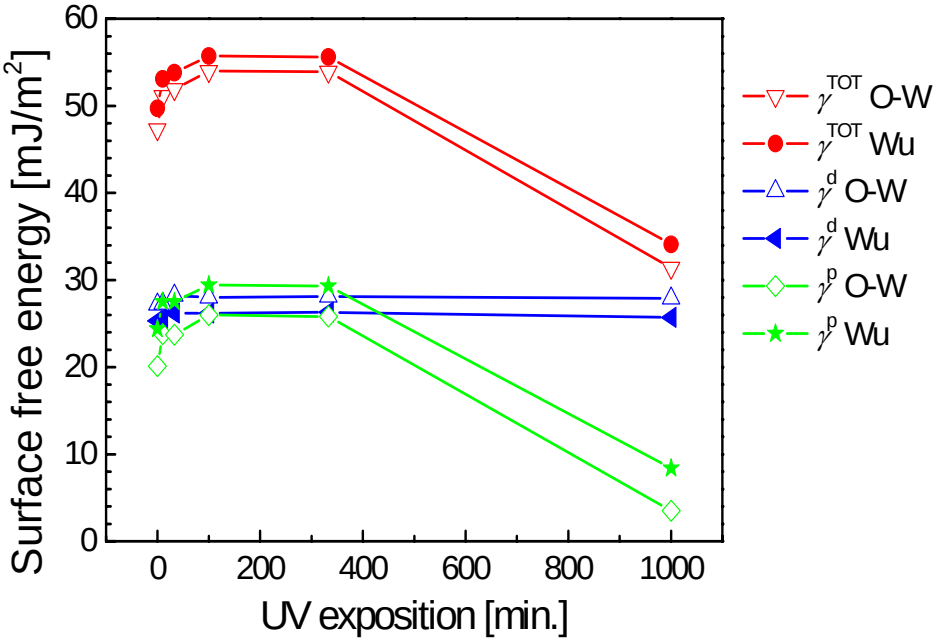

Figure 16: Dependence of the total surface free energy (γ^{TOT}) and its component (γ^{d} – dispersion part, γ^{p} – polar part) evaluated according Owens-Wendt and Wu method on time of UV exposition

3.3 MULTILAYERS ON THE BASIS OF TETRAVINYLSILANE

The single layer, bi-layered, and 10-layered films were deposited to investigate their optical properties by ellipsometry.

Single layer films deposited at a power set on 10, 20, 25, 50, and 70 W were characterized by spectroscopic ellipsometry to evaluate their thickness and the dispersion dependences of optical constants. The new set of single layer films is described in this Chapter for better comparison with multi-layered systems.

Dispersion curves for the refractive index are shown in Figure 17 and correspond to the single layer film, approximately 1 μm thick, deposited at different powers. The pp-TVS films were relatively well transparent and the dispersion curves for the extinction coefficient were not well separated according to the power used and thus not presented in this study. The dispersion dependence for the refractive index moved to higher values with enhanced power and the refractive index at a wavelength of 633 nm increased from 1.69 (10 W) to 2.08 (70 W). This behavior can be described by the Clausius-Mossotti relationship [44] and corresponds to an increased density of polarizable species in a-SiC:H alloy due to higher cross-linking of plasma polymer with enhanced power.

Two plasma polymers (pp-TVS deposited at a power of 10 and 25 W) of slightly different optical properties were selected to construct layered structures. The single layer films were subjected to RBS and ERDA spectroscopies to evaluate the elemental composition of a-SiC:H alloy influenced by RF power. The atomic concentrations corresponding to silicon (Si), carbon (C), and hydrogen (H) are given in Figure 18 for the two pp-TVS films deposited at a power of 10 and 25 W. The chemical composition of selected a-SiC:H alloys was not very different. The content of silicon was very similar, i.e., 5.8 at.% (10 W) and 7.5 at.% (25 W), while concentration of carbon increased by 12.1 at.% at an expense of hydrogen concentration (13.8 at.%) if a higher power of 25 W was used. The organic/inorganic character (expressed by carbon to silicon ratio) of the alloy was changed from 4.6 (10 W) to 5.2 (25 W).

Bi-layered films were constructed from a-SiC:H alloys deposited at a power of 10 and 25 W, where the first individual layer was prepared at a power of 10 W followed by the second layer prepared at a power of 25 W. For the reasons of sharp interface necessity a movable substrate shutter was used to deposit the ultrathin film at steady-state plasma conditions monitored by mass spectroscopy. It means that TVS plasma is switched on and switched off at the shutter covered the substrates. The shutter is removed outside the plasma zone when the concentration of plasma species is stabilized, i.e., 0.5-1 min after the plasma was switched on. The substrate shutter was used to change the RF power during deposition of the multilayer structure as well.

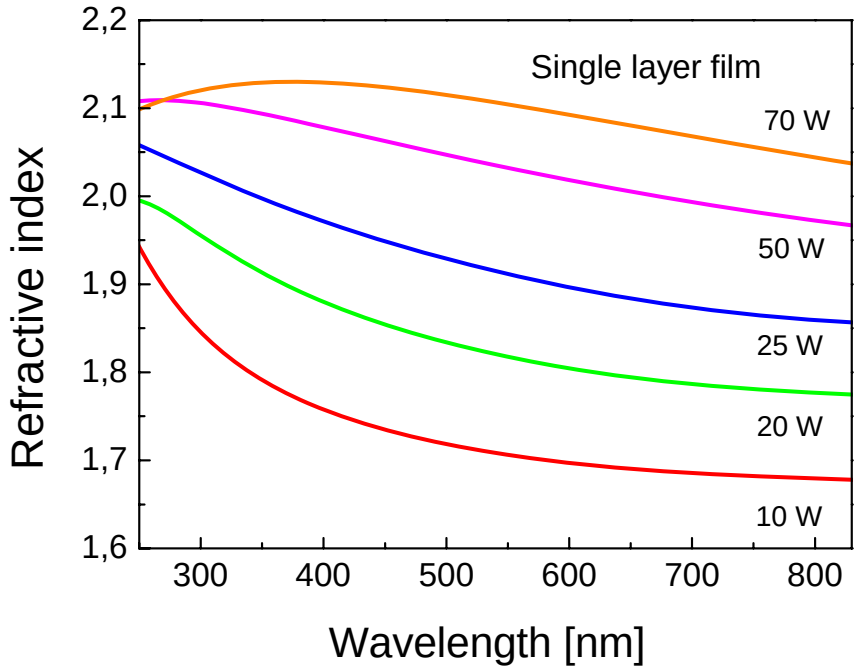

Figure 17: Dispersion curves for the refractive index of single layer film deposited at different RF powers

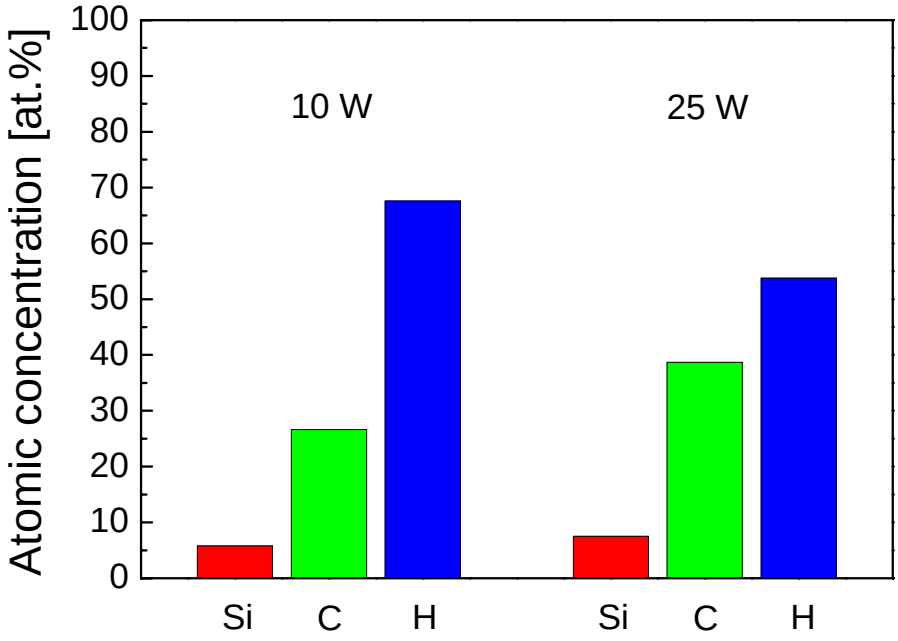

Figure 18: Elemental composition of single layer film deposited at an RF power of 10 W and 25 W

The thickness of individual layer was controlled by deposition time to reach a value of 500, 100, and 25 nm in three sets of specimens. The mean deposition rate calculated as a ratio between the layer thickness and deposition time was determined as 134 nm/min (10 W) and 168 nm (25 W) using the single film of thickness 964 nm (10 W) and 1065 nm (25 W). Ellipsometric spectra were analyzed using the model of bi-layered film that comprised the semi-infinite substrate, plasma polymer layer (10 W), plasma polymer layer (25 W), and the surface overlayer (Figure 19). This model resulted in good agreement between the experimental and simulated data enabling to distinguish the individual layers and evaluate their thickness and optical constants. The dispersion curves for the refractive index corresponding to the bottom (10 W) and upper (25 W) layers of different thickness are compared with those for the single layer film in Figure 20. There are no significant differences among the corresponding curves, except a region of very low wavelength, even in the case that ultrathin layers (25 nm) were used to construct the nanolayered structure. The accuracy of refractive index in UV range is lower due to increased absorption of deposited material at shorter wavelength. The thickness of individual layers was 521 nm (10 W) / 541 nm (25 W) in the bi-layered film if the expected values were 500 nm / 500 nm, next 98 nm (10 W) / 121 nm (25 W) if the expected values were 100 nm / 100 nm, and finally 33 nm (10 W) / 28 nm (25 W) if the expected values were 25 nm / 25 nm. These are promising results enabling us to construct more-layered films of controlled properties. However, the good results were obtained due to relatively sharp interfaces between the individual layers, where the interlayer thickness was <2 nm, in consequence of substrate shutter utilized to change RF power. A gradient interlayer was confirmed by ellipsometric analysis, if no shutter was used to eliminate non-steady-state plasma condition, resulting in more complicated sample model (more fitting parameters) and thus results of lower accuracy.

Figure 19: General scheme of the ellipsometric model for bi-layered films

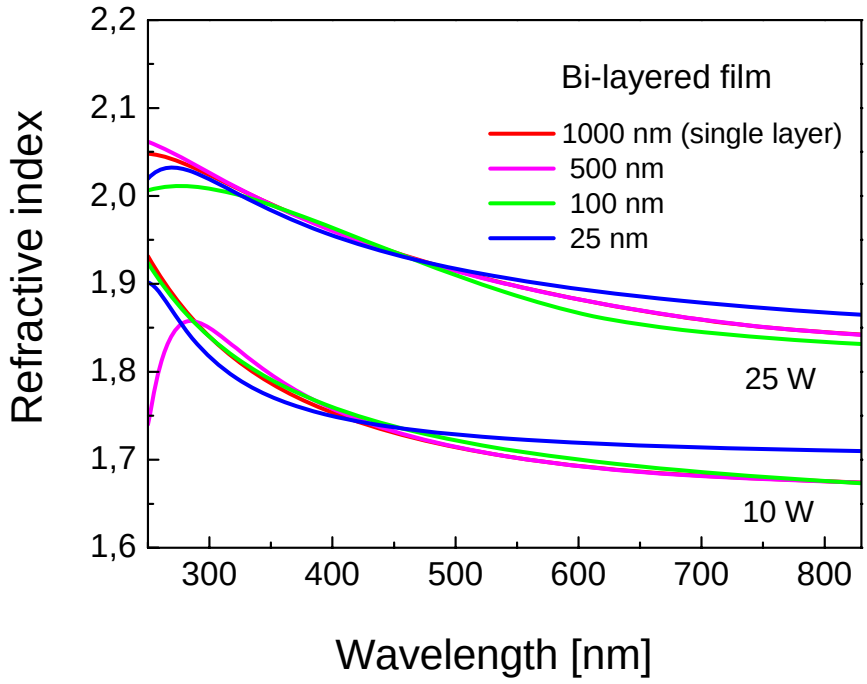

Figure 20: Dispersion curves for the refractive index of individual layers in bi-layered film. Dispersion curves corresponding to the individual layer of thickness 500, 100, and 25 nm are compared with that for single layer film

The 10-layered films were constructed from a-SiC:H alloys deposited at a power of 10 and 25 W using a layer-by-layer rotating system, where the first individual layer was prepared at a power of 10 W and the last layer prepared at a power of 25 W. The thickness of individual layer was controlled by deposition time to reach a value of 100 nm in one set of samples but 25 nm in another set of samples. Similar as for the bi-layered film, the sample model of 10-layered film used to simulate the ellipsometric spectra was consisted of the semi-infinite substrate, plasma polymer layer (10 W) and plasma polymer layer (25 W) repeated five times, and the surface overlayer. The five fitting parameters (Tauc-Lorentz formula) were the same for all the individual layers deposited at 10 W or respectively 25 W. This approach is realistic and resulted in a diminished number of fitting parameters. A good agreement between the experimental and simulated data enabled us to distinguish individual layers in the multilayer even in the case of 25 nm layer thickness. The dispersion curves for the refractive index were well separated into two groups corresponding to the layer deposited at 10 W and 25 W as given in Figure 21. The dispersion curves were compared with those for the single layer film and are almost identical for range of visible wavelength. The thickness of individual layer was 90-108 nm (10 W) and 98-114 nm (25 W) if the expected value was 100 nm and was 19-31 nm (10 W) and 19-27 nm (25 W) if the expected value was 25 nm.

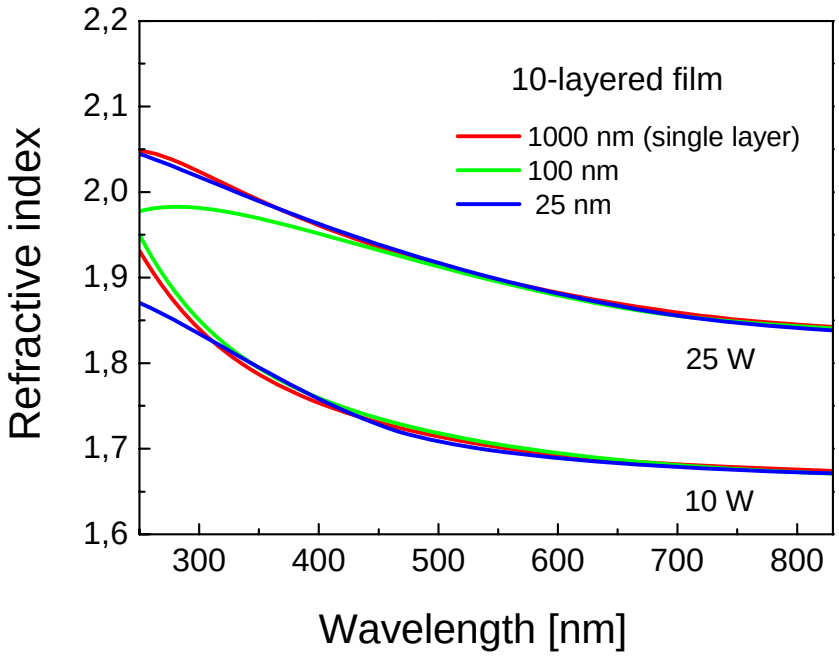

Figure 21: Dispersion curves for the refractive index of individual layers in 10-layered film. Dispersion curves corresponding to the individual layer of thickness 100 and 25 nm are compared with that for single layer film

The refractive index at a wavelength of 633 nm was compared for single layer, bi-layered, and 10-layered films as a function of the layer thickness in Figure 22. The dashed line corresponding to the refractive index of single layer film was used as a guide for eye. The refractive index of individual layer corresponds well to a value of 1.69 (10 W) or 1.87 (25 W) determined for thick single layer film. It means that there is no difference among optical properties of thick (1 μm) single layer film and ultrathin (25 nm) individual layer built in layered nanostructure. The mean deposition rate calculated from the layer thickness and deposition time as a function of the layer thickness is plotted in Figure 23. The mean value with error margin was used for 10-layered films. The dashed line corresponding to the deposition rate of single layer film was used as a guide for eye. The differences and increased error margin can be found for multilayered films with decreased layer thickness. This behavior can be explained by very short deposition time, used for deposition of individual layer (9-11 s was used to deposit 25 nm layer), which was influenced by manipulation with the substrate shutter. It is expected that the reproducibility of deposition rate in the case of nanolayers would be higher for plasma polymers of slower growth.

Spectroscopic ellipsometry was able to distinguish individual layers in the layered structure with sharp interfaces even if the thickness of individual layer was only about 25 nm. Therefore, nanolayered and gradual films of controlled optical properties can be developed for nanocomposite applications and optical devices.

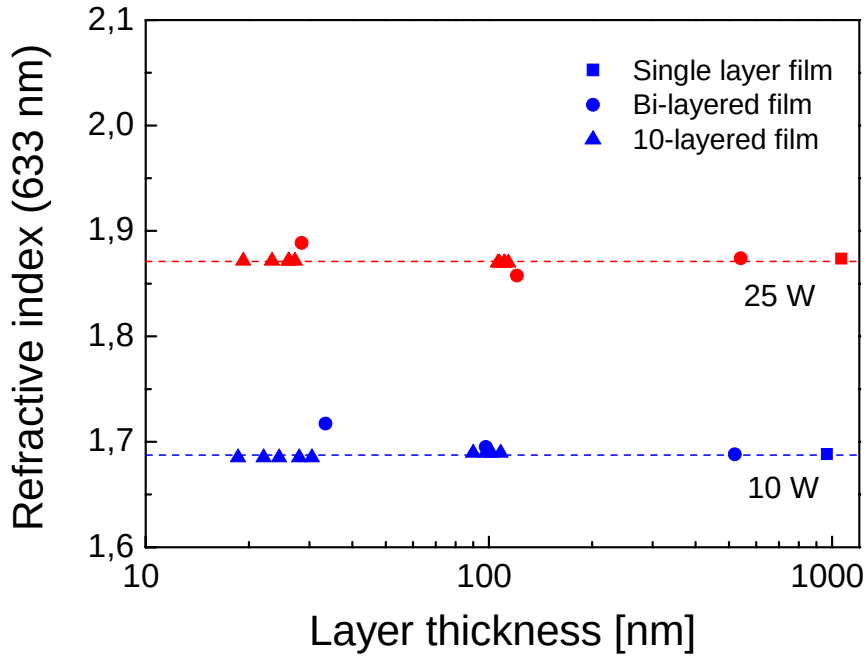

Figure 22: Refractive index at a wavelength of 633 nm as a function of layer thickness. Dashed line corresponding to the refractive index of single layer film is used as a guide for eye

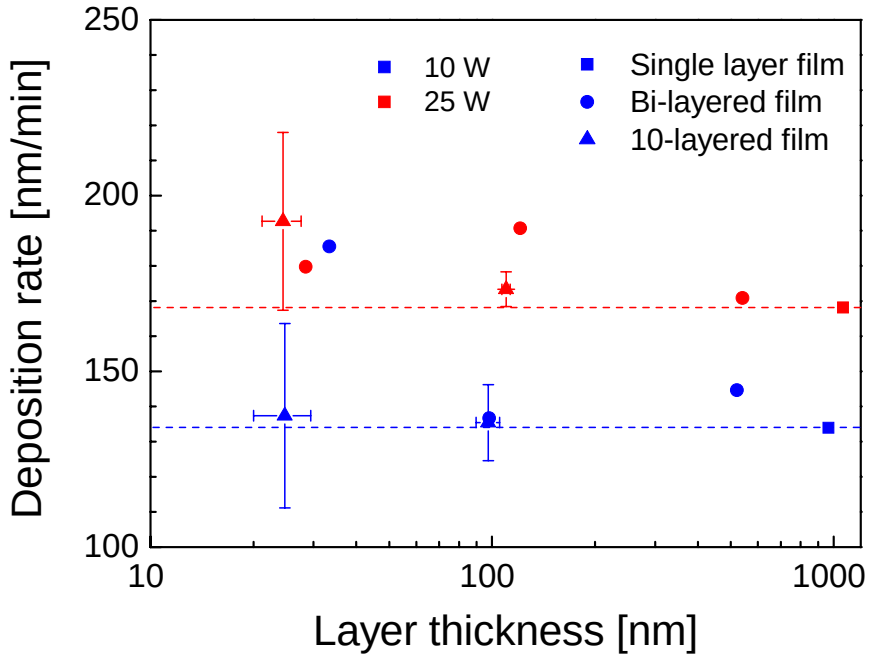

Figure 23: Deposition rate as a function of layer thickness. Dashed line corresponding to the deposition rate of single layer film is used as a guide for eye

4 CONLUSION

The aim of this work was research of plasma polymers on the basis of tetravinylsilane. The layers were prepared in low-pressure, low-temperature glow discharge by plasma-enhanced chemical vapor deposition. The influence of deposition conditions (effective power, RF power, monomer flow rate) on physical and chemical properties of deposited material was investigated.

Stable deposition conditions for preparation of pp-thin films from TVS were successfully determined. The set of samples deposited with the same monomer flow rate and different RF powers from 10 W – 70 W in the continual plasma regimes were prepared. Preparation reproducibility of pp-thin films has been proven as well as possibility to prepare materials with different properties by changing the deposition conditions, especially RF power. Influence of RF power on monomer fragmentation was observed by mass spectroscopy. Higher monomer fragmentation with increasing RF power occurred, as was expected, but in the case of atomic hydrogen.

The dispersion curves evaluated from spectroscopic ellipsometry were well separated according to the power used and the pp-TVS films were relatively well transparent. The dispersion dependence for the refractive index moved to higher values with enhanced power and the refractive index at a wavelength of 633 nm increased from 1.69 (10 W) to 2.08 (70 W). This behavior corresponds to an increased density of polarizable species in a-SiC:H alloy due to higher cross-linking of plasma polymer with enhanced power. Extinction coefficient increased towards infra-red area with increased RF power used during deposition. Energy gap, evaluated from ellipsometry measurements, decreased with enhanced power from 2.01 eV (10 W) to 1.16 eV (70 W), so material was more conductive with increasing RF power.

The FTIR spectra of pp-TVS layers were compared and discussed depending on the used RF power. Absorption bands connected with vinyl groups decreased with increasing RF power, as well as absorption bands assigned to groups containing oxygen, like C=O, OH, Si-O-C and Si-O-Si. It confirms lower crosslinking of plasma polymer prepared at lower RF power and so easier penetrating of atmospheric oxygen into prepared layer, lower fragmentation of monomer at lower RF powers and so higher content of vinyl groups in the plasma polymer.

Atomic concentration of layers, determined by RBS and ERDA methods, correlates well with FTIR measurements. Concentration of particular elements can be well controlled by RF power. The hydrogen content generally decreased with increasing RF power, from 64 % (10 W) to 40 % (70 W). Concentration of carbon increased with increasing RF power from 25 % (10 W) to 53 % (70 W). Oxygen concentration generally decreases slightly with increasing RF power, from 5 % (10 W) to almost 0 % (70 W). Silicon concentration can be considered as constant. With increasing RF power, element ratio C/Si generally increases from 5 to 7 for 10 W and 70 W respectively. Ratio C/Si expresses the change in organic-inorganic character of material. Material gains more organic character with increasing RF

power in the depth level of samples. Predisposition of pp-layers to oxidation can be expressed by element ratio O/Si, which decreases with increasing RF power. Samples prepared at lower RF powers are more subject to atmospheric degradation. XPS measurements confirmed growth of carbon concentration with increasing RF power at an expense of oxygen and silicon concentration.

The surface of pp-thin films, pursued by AFM microscopy, is indented and mainly formed by rounded shapes with height up to tens of nanometers. Evaluated Root Means Square (RMS) roughness increased with enhanced power from 3.4 nm (10 W) to 22 nm (70 W). Mechanical properties of pp-layers can be also controlled by deposition conditions, as was proven by nanoindentation measurements. Young modulus and hardness increased with enhanced RF power in range of 16.8 GPa (10 W) – 76.9 GPa (70 W) and 2.91 GPa (10 W) – 12.56 GPa (70 W), respectively.

Wettability measured by contact angle method increased with increasing RF power as well as the total surface free energy evaluated according to Owens-Wendt and Wu methods. It means that pp-TVS thin films prepared at lower RF powers are less hydrophilic than films prepared at higher RF powers.

Mechanical and chemical properties of single layer films prepared at continual regime can be tailored according to our demands by changing deposition conditions. Layers prepared at higher RF power are more cross-linked, formed more by carbon than by silicon and oxygen. Hence the layers are more stable against post-deposition degradation and aging on the atmosphere and have better mechanical properties than layers prepared at lower RF powers.

One chapter was devoted to UV degradation of thin films prepared in continual regime. Plasma-polymerized tetravinylsilane (pp-TVS) films were deposited on silicon wafers at RF power of 10 W. Two batches, each of six samples, with a film thickness of 0.1 μm and 0.5 μm, respectively, were deposited using the same deposition conditions. The as-deposited films were subjected to UV irradiation at ambient conditions for different times ranging from 10 to 1000 min. Modifications of the chemical and physical properties of the irradiated films were investigated in comparison with those of the reference sample (as-deposited film). The changes in the UV-irradiated films mostly increased with prolonged UV exposition time, reaching their maxima at 1000 min, and had the same character for both batches. The chemical composition of the as-deposited film can be expressed as a-$SiC_{4.9}$:$H_{6.6}$ using RBS/ERDA analyses and was significantly changed into a-$SiO_{2.0}C_{0.5}$:$H_{0.6}$ after 1000 min of UV irradiation, i.e., oxidation of the polymer and a very considerable reduction of carbon and hydrogen concentrations. The FTIR spectra confirmed oxidation of the plasma polymer network forming stronger Si–O–C bonding species at the expense of weaker Si–C groups, accompanied by higher cross-linking resulting in an increase of mechanical constants (Young's modulus, hardness) and density by 20-25%. The RMS roughness of the irradiated films decreased from 0.41 to 0.12 nm with prolonged UV exposition time, and the film thickness was reduced by 50% at 1000 min of UV irradiation. The wettability of the irradiated films increased during 333 min of UV exposition but decreased abruptly at 1000 min in

correspondence with the concentration of polar groups (OH, C=O). The optical constants of the irradiated pp-TVS films were significantly influenced by the oxidation process and the refractive index decreased by 17% (633 nm), while the extinction coefficient dropped by as much as 95% (250 nm). The most intensive aging effect was observed for the reference sample (as-deposited film): here the chemical composition changed to a-$SiO_{2.1}C_{4.7}$:$H_{6.4}$ after 134 days, evidencing the oxidation effect. Longer UV exposition resulted in a smaller aging effect, with the 1000-min-UV-irradiated film appearing stable for 134 days.

Multilayered structures on the basis of plasma polymers were also prepared as bi-layered, and 10-layered films using continuous RF plasma. Bi-layered and 10-layered films were constructed from a-SiC:H alloys deposited at a power of 10 and 25 W, where the first individual layer was prepared at a power of 10 W followed by the second layer prepared at a power of 25 W, using layer-by-layer rotating system. The thickness of individual layer was controlled by deposition time to reach a value of 500, 100, and 25 nm. Multilayered systems were analyzed by spectroscopic ellipsometry to find out if the individual layers can be distinguished and characterized with respect to their thickness and optical constants. Spectroscopic ellipsometry was able to distinguish individual layers in the layered structure with sharp interfaces even if the thickness of individual layer was only about 25 nm. The dispersion curves of multilayers were compared with those for the single layer film and are almost identical for range of visible wavelengths. It means that there is no difference among optical properties of thick (1 μm) single layer film and ultrathin (25 nm) individual layer built in layered nanostructure. Therefore, nanolayered and gradual films of controlled optical properties can be developed for nanocomposite applications and optical devices.

5 REFERENCES

[1] **Langmuir, I.** *Oscillations in ionized gases*. Proceedings of the National Academy of Sciences of the United States of America, 1928, vol. 14, pp. 627 – 637.

[2] **Yasuda, H.** *Plasma Polymerization.* New York: Academic Press Inc., 1985.

[3] **Biederman, H.** Plasma Polymer Films. London: Imperial College Press, 2004.

[4] **Biederman, H., Slavínská, D.** *Plasma polymer films and their future prospects.* Surface and Coatings Technology, 2000, vol. 125, pp. 371 – 376.

[5] **Shi, F.F.** *Review Recent advances in polymer thin films prepared by plasma polymerization, Synthesis, structural characterization, properties and applications.* Surface and Coatings Technology, 1995, vol. 82, pp. 1 – 15.

[6] **Bogaerts, A., Neyts, E, Gijbels, R., Mullen, J.** *Gas discharge plasmas and their applications*. Spectrochimica Acta Part B, 2001, vol. 57, pp. 609 – 658.

[7] **Grundmeier, G., Thiemann, P., Carpentier, J., Barranco, V.** *Tailored thin plasma polymers for the corrosion protection of metals*. Surface and Coatings Technology, 2003, vol. 174–175, pp. 996 – 1001.

[8] **Grüniger, A., Bieder, A., Sonnenfeld, A., Ph. von Rohr, R., Müller, U., Hauert, R.** *Influence of film structure and composition on diffusion barrier performance of SiO_X thin films deposited by PECVD*. Surface and Coatings Technology, 2006, vol. 14 – 15, pp. 4564 – 4571.

[9] **Bieder, A., Grüniger, A., Ph. von Rohr, R.** *Deposition of SiO_x diffusion barriers on flexible packaging materials by PECVD*. Surface and Coatings Technology, 2005, vol. 200, pp. 928 – 931.

[10] **Vetter, J., Barbezat, G., Crummenauer, J., Avissar, J.** *Surface treatment selections for automotive applications*. Surface and Coatings Technology, 2005, vol. 200, pp. 1962 – 1968.

[11] **Favia, P., Sardella, E., Gristina, R., D'Agostino, R.** *Novel plasma processes for biomaterials: micro-scale patterning of biomedical polymers*. Surface and Coatings Technology, 2005, vol. 169 – 170, pp. 707 – 711.

[12] **Favia, P., Lopez, L.C., Sardella E., Gristina R., Nardulli M., D'Agostino R.** *Low temperature plasma processes for biomedical applications and membrane processing*. Desalination, 2006, vol. 199, pp. 267 – 7270.

[13] **Kim, H.J., Shao, Q., Kim, Y-H.** *Characterization of low-dielectric-constant SiOC thin films deposited by PECVD for interlayer dielectrics of multilevel interconnection*. Surface and Coatings Technology, 2003, vol. 171, pp. 39 – 45.

[14] **Borvon, G., Goullet, A., Mellhaoui, X., Charrouf, N., Granier, A.** *Electrical properties of low-dielectric-constant films prepared by PECVD in O2/CH4/HMDSO*. Materials Science in Semiconductor Processing, 2002, vol. 5, pp. 279 – 284.

[15] **Navamathavan, R., Choi, C.H.** *Plasma enhanced chemical vapor deposition of low dielectric constant SiOC(–H) films using MTES/O2 precursor*. Thin Solid Films, 2007, vol. 515, pp. 5040 – 5044.

[16] **Lee, H., Oh, K., Choi, C.** *The mechanical properties of the SiOC(-H) composite thin films with a low dielectric constant*. Surface & Coatings Technology, 2002, vol. 171, pp. 296 – 301.
[17] **Behnisch, J., Tyczkowski, J., Gazicki, M., Pela, I, Ledzion, R.** *Formation of hydrophobic layers on biologically degradable polymeric foils by plasma polymerization*. Surface and Coatings Technology, 1998, vol. 98, pp. 872 – 874.
[18] **Lee, J.H., Jeong, C.H., Lim, J.T., Zavaleyev, V.A., Kyung, S.J., Yeom, G.Y.** *Characteristics of a multilayer $SiO_x(CH)_yN_z$ film deposited by low temperature plasma enhanced chemical vapor deposition using hexamethyldisilazane/Ar/N_2O*. Japanese Journal of Applied Physics*, 2006, vol.* 45, pp. 8430 – 8434.
[19] **Zhang, Z., Wagner, T., Sigle, W., Schulz, A.** *EELS study of a multilayered SiO_x and SiO_xC_y film prepared by plasma-enhanced chemical vapor deposition*. Journal of Materials Research, 2006, vol. 21, pp. 608 – 612.
[20] **Joinet, M., Pouliquen, S., Thomas, L., Teyssandier, F., Aliaga D.** *Comparison between single and multilayered a-SiC:H coatings prepared by multi-frequency PACVD: Mechanical properties*. Surface and Coatings Technology, 2008, vol. 202, pp. 2252 – 2256.
[21] **Cech V.** *Plasma polymer film as a model interlayer for polymer composites*. IEEE Transactions on Plasma Science, 2006, vol. 34**,** pp. 1148 – 1155.
[22] **Gujrathi, S.C., Poitras, D., Klemberg-Sapieha, J.E., Martinu, L.** *Erd-Tof characterization of silicon-compound multilayer and graded-index optical coatings*. Nuclear Instruments & Methods in Physics Research, Section B, 1996, vol. 118, pp. 560 – 565.
[23] **Prikryl, R, Čech, V., Hedbavny, P., Inagaki, N.** *Novel plasma reactor with bottom rotary electrode for Plasma-enhanced chemical vapor deposition of nanostructured films*. Proceedings of 17th symposium on plasma chemistry. Toronto, Canada, Centre for Advanced coatings Technology, University of Toronto, 2005, p. 1 – 6.
[24] **Prikryl, R, Čech, V., Studynka, J.** *Burning conditions of non-thermal Ar-plasma at continuous and pulsed mode*. Czechoslovak Journal of Physics, 2006, Vol. 56, Supplement 2, B1320 – B1325.
[25] Catalog 2002 – 2004 Vacuum Technology, Pfeiffer Vacuum, May 2002.
[26] TriScroll™ 300 Series Vacuum Pump – Varian, Instalation and operation manual, revision M, Manual No. 699904265.
[27] **Bunshah, R.** Handbook of Deposition Technologies for Films and Coatings – Science, Technology and Applications. New Jersey: Noyes Publications Park Ridge, 1994.
[28] **Balkova, R., Zemek, J., Cech, V., Vanek, J., Prikryl, R.** *XPS study of siloxane plasma polymer films.* Surface & Coating Technology, 2003, vol. 174-175, pp 1159-1163.

[29] **Macková A., Peřina V., Švorčík V, Zemek J.** *RBS, ERDA and XPS study of Ag and Cu diffusion in PET and PI polymer foils.* Nuclear Instruments and Methods in Physics Research B, 2005, vol. 240, pp 303-307.
[30] **Cech, V., Studynka, J., Conte, N., Perina, V.** *Physico-chemical properties of plasma-polymerized tetravinylsilane.* Surface & Coatings Technology, 2007, vol. 201, pp 5512-5517.
[31] **Wu, S.** *Polymer Interface and Adhesion.* New York: Marcel Dekker, Inc., 1982. ISBN 0-8247-1533-0.
[32] **DataPhysics Instrument 1998.** *Operating manual Data Physics OCA.* Filderstadt, Germany : DataPhysics Intrument 1998
[33] **Caha, O., Meduňa, M.** *X-ray diffraction on precipitates in Czochralski-grown silicon.* Physica B: Condensed Matter, 2009, vol. 404, Issues 23 – 24, pp 4626-4629.
[34] **Trivedi, R.** *Study of thin-film surfaces*, Brno, 2010, 116 p. Dissertation work at the institute of Materials Science, Faculty of Chemistry, Brno University of Technology. Supervisor prof. RNDr. Vladimír Cech, Ph.D.
[35] **Studýnka, J.** *Preparing of layers and multilayered structures of plasma polymers.* Brno, 2008. 125 p. PhD Thesis at Faculty of Chemistry Brno University of Technology, Institute of Materials Chemistry. Supervisor prof. RNDr. Vladimír Čech, Ph.D. [in Czech].
[36] **Cech, V., Studynka, J., Conte, N., Perina, V.** *Physico-chemical properties of plasma-polymerized tetravinylsilane.* Surface & Coatings Technology, 2007, vol. 201, pp 5512-5517.
[37] **Verdonck, P., De Roest, D., Kaneko, S., Caluwaerts, R., Tsuji, N., Matsushita, K., Kemeling, N., Travaly, Y., Sprey, H., Schaekers, M., Beyer, G.** *Characterization and optimization of porogen-based PECVD deposited extreme low-k materials as a function of UV-cure time.* Surface and Coating Technology, 2007, vol. 201, pp. 9264 – 9268.
[38] **Mitchell, B. S.** Materials Engineering and Science for Chemical and Materials Engineers, Wiley, New Jersey 2004, pp. 851.
[39] **Weibel, D. E., Michels, Horowitz, F., Cavalheiro, R. da S., Mota, G. V. da S.** *Ultraviolet-induced surface modification of polyurethane films in the presence of oxygen or acrylic acid vapours.* Thin Solid Films, 2009, vol. 517, pp. 5489 – 5495.
[40] **Zhao, X., Li, Z., Chen, Y., Shi, L., Zhu, Y.** *Solid-phase photocatalytic degradation of polyethylene plastic under UV and solar light irradiation.* Journal of Molecular Catalysis A: Chemical, 2007, vol. 268, pp. 101 – 106.
[41] **Cech, V., Studynka, J., Cechalova, B., Mistrik, J., Zemek, J.** *Correlation between mechanical, optical and chemical properties of thin films deposited by PECVD*. Surface & Coatings Technology, 2008, vol. 202, pp. 5572 – 5575.
[42] **D.A.G. Bruggeman**, Ann. Phys. 24 (1935) 636 – 791.
[43] **Øiseth, S. K, Krozer, A., Lausmaa, J., Kasemo, B.** *Ultraviolet light treatment of thin high-density polyethylene films monitored with quartz crystal*

microbalance. Journal of Applied Polymer Science, 2004, vol. 92, pp. 2833 – 2839.

[44] **Tompkins, H., Irene, E.** *Handbook of Ellipsometry*. Norwich: William Andrew Publishing, 2005.

Author's biography

Ing. Soňa Kontárová (nee Lichovníková)

Born

24.4.1982	Opava

Education

1998 – 2002	Secondary study: Silesian Grammar school in Opava
2002 – 2007	Masters study: Brno University of Technology, Faculty of Chemistry branch: Material Science and Technology degree: Ing.
2007 –	Doctoral study: Brno University of Technology, Faculty of Chemistry branch: Chemistry, Technology and Properties of Materials

Selected publications

LICHOVNÍKOVÁ, S.; STUDÝNKA, J.; ČECH, V. Wettability of plasma-polymerized vinyltriethoxysilane film. *Chemical Papers.* 2009. 63(4). p. 479 - 483. ISSN 0366-6352.

ČECH, V.; LICHOVNÍKOVÁ, S.; SOVA, J.; STUDÝNKA, J. Surface free energy of silicon-based plasma polymer films. In *Silanes and other coupling agents.* VSP. 2009. p. 333 - 348. ISBN 978-90-04-16591-5.

KONTÁROVÁ, S.; PEŘINA, V.; ČECH, V. Plasma polymer multilayers of organosilicones and their optical properties controlled by RF power. In *Surface & Coatings Technology,* 2011, In press

ČECH, V., LICHOVNÍKOVÁ, S.; TRIVEDI, R.; PERINA, V.; ZEMEK, J.; MIKULIK, P.; CAHA, O. Plasma polymer films of tetravinylsilane modified by UV irradiation. In *Surface & Coatings Technology,* 2010, Volume 205, Supplement 1, S177 – S181

ABSTRACT

This study is aimed at the basic research of plasma polymer films and an influence of deposition conditions on structure and properties of single-layer films and multilayers prepared by PE CVD method. Single layer and multilayered a-SiC:H films were deposited on silicon wafers from tetravinylsilane monomer (TVS) at different powers. The films were investigated extensively by spectroscopic ellipsometry, nanoindentation, atomic force microscopy (AFM), X-ray photoelectron spectroscopy (XPS), Rutherford Backscattering Spectrometry (RBS), X-ray reflectivity, Fourier Transform Infrared Spectroscopy (FTIR) and contact angle measurements to observe their optical, mechanical and chemical properties. The influence of the deposition condition on the physicochemical properties of pp-TVS films was revealed and quantified. Single layers were also exposed to UV light as post-deposition treatment to investigate aging effects and the influence of UV irradiation on their physical and chemical properties. Multilayered structures (bi-layered and 10-layered plasma polymerized films) of individual layer thickness down to 25 nm were successfully deposited and characterized by ellipsometric spectroscopy. Materials with tailored properties can be developed for nanocomposite applications and optical devices.

ABSTRAKT

Tato studie je zaměřena na základní výzkum tenkých vrstev plazmových polymerů a vliv depozičních podmínek na strukturu a vlastnosti jednotlivých vrstev a multivrstev připravených pomocí metody PE CVD. Jednotlivé vrstvy a multivrstvy a-SiC:H byly deponovány na křemíkové substráty z monomeru tetravinylsilanu (TVS) při různých výkonech. Vrstvy byly rozsáhle zkoumány pomocí spektroskopické elipsometrie, nanoindentace, mikroskopie atomárních sil (AFM), rentgenové fotoelektronové spektroskopie (XPS), spektroskopie Rutherfordova zpětného rozptylu (RBS), rentgenové reflektivity, Fourierovy transformační infračervené spektroskopie (FTIR) a měření kontaktního úhlu, pro zjištění jejich optických, mechanických a chemických vlastností. Byl zkoumán a prokázán vliv depozičních podmínek na fyzikálně-chemické vlastnosti pp-TVS vrstev. Jednotlivé vrstvy byly v rámci po-depoziční úpravy vystaveny UV záření a byl zkoumán účinek stárnutí a vliv UV záření na jejich fyzikální a chemické vlastnosti. Multivrstevnaté struktury (plazmaticky polymerizované 2-vrstvy a 10-ti-vrstvy) s tloušťkou jednotlivých vrstev od 0,5 μm do 25 nm byly úspěšně deponovány a charakterizovány pomocí elipsometrické spektroskopie. Na základě získaných poznatků je možné připravit materiály s vlastnostmi upravenými podle požadavků pro využití v nanokompozitních aplikacích a optických zařízeních.